Comparison of different cylindrical shell theories for stability of nanocomposite piezoelectric separators containing rotating fluid considering structural damping

H. Rahimi Pour [*1], A. Ghorbanpour Arani [1,2] and G.A. Sheikhzadeh [1]

[1] *Faculty of Mechanical Engineering, University of Kashan, Kashan, Iran*
[2] *Institute of Nanoscience& Nanotechnology, University of Kashan, Kashan, Iran*

Abstract. Rotating fluid induced vibration and instability of embedded piezoelectric nano-composite separators subjected to magnetic and electric fields is the main contribution of present work. The separator is modeled with cylindrical shell element and the structural damping effects are considered by Kelvin–Voigt model. Single-walled carbon nanotubes (SWCNTs) are used as reinforcement and effective material properties are obtained by mixture rule. The perturbation velocity potential in conjunction with the linearized Bernoulli formula is used for describing the rotating fluid motion. The orthotropic surrounding elastic medium is considered by spring, damper and shear constants. The governing equations are derived on the bases of classical shell theory (CST), first order shear deformation theory (FSDT) and sinusoidal shear deformation theory (SSDT). The nonlinear frequency and critical angular fluid velocity are calculated by differential quadrature method (DQM). The detailed parametric study is conducted, focusing on the combined effects of the external voltage, magnetic field, visco-Pasternak foundation, structural damping and volume percent of SWCNTs on the stability of structure. The numerical results are validated with other published works as well as comparing results obtained by three theories. Numerical results indicate that with increasing volume fraction of SWCNTs, the frequency and critical angular fluid velocity are increased.

Keywords: viscoelastic separators; rotating fluid; different shell theories; orthotropic viscoelastic medium; DQM

1. Introduction

The prevalent engineering applications of a kind of separators containing rotating fluid flow are coming to be ever more obvious. Rotational fluid flow can leads to significant changes in stability behavior of the structure. However, in this paper, the separator conveying rotating fluid is modeled with a cylindrical shell element to analyze the stability of it.

Piezoelectric cylindrical shells have great application in different industries. In this regards, there are many works for mathematical modelling and mechanical analysis of them. Dong and Wang (2006) reported the result of an investigation into wave propagation in orthotropic laminated piezoelectric cylindrical shells in hydrothermal environment. Sofiyev (2011) focused on the thermal buckling analysis of functionally graded material (FGM) shells resting on the two-parameter elastic foundation. Amabili (2011) presented a comparative study on the nonlinear forced vibration of laminated circular cylindrical shells using different cylindrical shell theories. SSDT was used by Mantari and Guedes Soares (2014) for the bending analytical solution of FGM shells. An accurate solution approach based on the FSDT was developed by Yang *et al*.

(2015) for the free vibration and damping analysis of thick sandwich cylindrical shells with a viscoelastic core under arbitrary boundary conditions. The dynamic behavior of moderately thick FGM embedded cylindrical shell based on the FSDT was studied by Bahadori and Najafizadeh (2015) using DQM. Sofiyev (2016) investigated the non-linear free vibration of functionally graded (FG) orthotropic cylindrical shells taking into account the shear stresses.

None of the above works has analyzed the nano-composite structures. For obtaining the equivalent characteristic of the nanocomposite structures, there are many methods such as Mori-Tanaka, micro-mechanic, mixture and etc. Vibration analysis of SWCNTs reinforced composites was presented by Formica *et al*. (2010) employing Eshelby–Mori–Tanaka approach. Free vibration of continuous grading fiber reinforced (CGFR) annular plates on an elastic foundation, based on the three-dimensional theory of elasticity, for different boundary conditions at the circular edges was investigated by Tahouneh and Ceruti (2013) using DQM. Tahouneh and Yas (2014) presented 3D elasticity solution for free vibration analysis of 2D continuously graded carbon nanotube-reinforced (CGCNTR) annular plates resting on a two-parameter elastic foundation based on Eshelby-Mori-Tanaka Scheme. Static stresses analysis of carbon nano-tube reinforced composite (CNTRC) cylinder made of poly-vinylidene fluoride (PVDF) was investigated by Ghorbanpour Arani *et al*. (2015a) based on Mori–Tanaka theory. Using micro-mechanical model, Ghorbanpour Arani

---

∗Corresponding author, Ph.D.,
  E-mail: h.rahimipour@nioc.ir

et al. (2013a, 2015b) studied nonlinear vibration, stress analysis and stability of embedded piezoelectric composite cylindrical shell reinforced by nanotubes. An accurate buckling analysis for piezoelectric fiber-reinforced composite (PFRC) cylindrical shells subjected to combined loads comprising compression, external voltage and thermal load was presented by Sun *et al.* (2016) utilizing the Mixture rule. Eshelby-Mori-Tanaka approach was used by Tahouneh (2016) for 3-D elasticity solution for free vibration analysis of continuously graded carbon nanotube-reinforced (CGCNTR) rectangular plates resting on two-parameter elastic foundations. Kumar and Srivastava (2016) compared the effective elastic properties of CNT- and graphene-based nanocomposites using 3-D nanoscale representative volume element (RVE) based on continuum mechanics using finite element method (FEM).

Stability analysis of cylindrical shells containing internal and rotating fluid flow has been presented by many researchers. Dowell *et al.* (1974) studied aeroelastic stability of cylindrical shells subjected to a rotating flow. Païdoussis *et al.* (1992) presented a study of the effect of some of the system parameters on internal and angular-flow-induced instabilities of clamped-clamped or cantilevered cylindrical shells in coaxial conduits. A linear stability analysis was presented by Chen and Bert (1977) for a thin-walled, circular cylindrical shell of orthotropic material conveying a swirling flow. Flexible cantilever pipes conveying fluids with high velocity were analysed by Ganesan and Ramu (1995) for their dynamic response and stability behaviour. Amabili *et al.* (2001) studied nonlinear stability of circular cylindrical shells in annular and unbounded axial flow. Cortelezzi *et al.* (2004) investigated flutter instability of rotating shells with aco-rotating axial flow. By coupling the Donnell–Mushtari shell equations to an analytical inviscid fluid solution, the linear dynamics of a rotating cylindrical shell with a corotating axial fluid flow was studied by Gosselin and Païdoussis (2009). Numerical analysis of the stability of stationary and rotating cylindrical shells interacting with a fluid flowing and rotating inside them was presented by Bochkarev and Matveenko (2012a). In another work by the same authors (2012b, 2013a, b), the stability and dynamic of stationary orrotating elastic

circular cylindrical shells interacting with a fluidflow having both the axial and circumferential components of velocity was analyzed. Viscous fluid induced nonlinear free vibration and instability analysis of a functionally graded carbon nanotube-reinforced composite (CNTRC) cylindrical shell integrated with two uniformly distributed piezoelectric layers on the top and bottom surfaces of the cylindrical shell were presented by Ghorbanpour Arani *et al.* (2015c). Axially flowing and rotating fluid-particle mixture induced vibration and instability of a sandwich cylindrical shell were investigated by Ghorbanpour Arani *et al.* (2016) based on Mindlin shell theory and using DQM.

However, to date, no report has been found in the literature on stability analysis of separators conveying rotating fluid flow. Motivated by these considerations, in order to improve optimum design of separators, we aim to investigate the nonlinear vibration and instability of embedded piezoelectric nano-composite separators containing rotating fluid subjected to magnetic and electric fields. To describe the motion of the rotating fluid, the perturbation velocity potential function in wave equation for the case of small perturbations is used. The separator is reinforced with the SWCNTs which the equivalent material properties are obtained by Mixture rule. The nonlinear formulation is based on the CST, FSDT and SSDT considering structural damping based on Kelvin–Voigt model. Nonlinear frequency and critical fluid angular velocity of the structure are calculated using DQM. The effects of the external voltage, magnetic field, visco-Pasternak foundation, structural damping and volume percent of SWCNTs on the vibration and instability behavior of the structure are disused in detail.

2. Mixture rule

A piezoelectric separator reinforced with SWCNTs containing fluid is shown in Fig. 1. The structure is surrounded by an elastic medium which is simulated by spring, damper and shear constants. The cylindrical coordinate is considered in the middle surface of shell in which x, θ and Z represent the axial, circumferential and
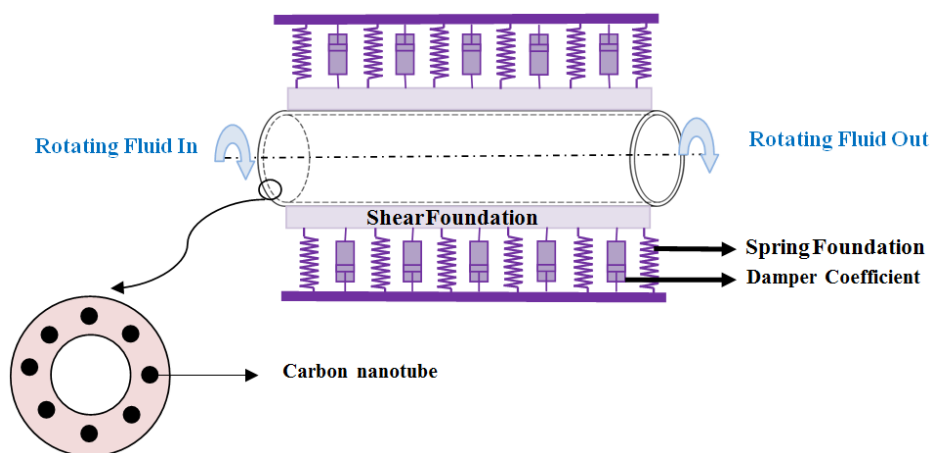

Fig. 1 A schematic figure for piezoelectric nano-composite separator conveying rotating fluid

radial directions, respectively.

According to mixture rule, the effective Young and shear moduli of nano-composite structure can be expressed as (Lei *et al.* 2014)

$$E_{11} = \eta_1 V_{CNT} E_{r11} + (1 - V_{CNT}) E_m, \qquad (1)$$

$$\frac{\eta_2}{E_{22}} = \frac{V_{CNT}}{E_{r22}} + \frac{(1 - V_{CNT})}{E_m}, \qquad (2)$$

$$\frac{\eta_3}{G_{12}} = \frac{V_{CNT}}{G_{r12}} + \frac{(1 - V_{CNT})}{G_m}, \qquad (3)$$

where E_{r11}, E_{r22} and G_{r11} indicate the Young's moduli and shearmodulus of SWCNTs, respectively, E_m and G_m represent the Young's moduli and shear modulus the matrix; η_j ($j = 1, 2, 3$) is the SWCNTs efficiency parameter; V_{CNT} and V_m are the volume fractions of the CNTs and matrix, respectively, which are

$$V_{CNT} = \frac{w_{CNT}}{w_{CNT} + (\rho_{CNT} / \rho_m) - (\rho_{CNT} / \rho_m) w_{CNT}}, \qquad (4)$$
$$V_m = 1 - V_{CNT},$$

where w_{CNT}, ρ_m and ρ_{CNT} are the mass fraction of the SWCNTs, the densities of the matrix and SWCNTs, respectively. Similarly, the density (ρ) of the structure can be obtained as follows

$$\rho = V_{CNT} \rho_r + V_m \rho_{m,}, \qquad (5)$$

where v_{r12} and v_m are Poisson's ratios of the SWCNT and matrix, respectively.

3. Piezoelectric material basic equations

In piezoelectric material, the constitutive equation includes stresses σ and strains ε tensors on the mechanical side, as well as flux density D and field strength E tensors on the electrostatic side, which may be combined with each other as follows (Ghorbanpour Arani *et al.* 2013b)

$$\sigma_{ij} = C_{ijkl} \varepsilon_{kl} - e_{ijm} E_m, \qquad (6)$$

$$D_i = e_{ijm} \varepsilon_{jm} + \in_{im} E_m, \qquad (7)$$

where C_{ijkl}, e_{ijm}, $\in_{im}$ are elastic constants, piezoelectric constants, dielectric constants, respectively, which can be determined for separator reinforced with SWCNT from Mixture's rule. In addition, E_m ($m = x, \theta, z$) representing electric field which can be defined as a function of electric potential as

$$E_x = -\frac{\partial \phi}{\partial x}, \ E_\theta = -\frac{\partial \phi}{R \partial \theta}, \ E_z = -\frac{\partial \phi}{\partial z}. \qquad (8)$$

The electric potential distribution in the thickness direction of the piezoelectric separator can be assumed as

follows which satisfying the Maxwell equation (Ghorbanpour Arani *et al.* 2015c)

$$\Phi(x, \theta, z, t) = -\cos\left(\frac{\pi z}{h}\right) \phi(x, \theta, t) + \frac{2 V_0 z}{h}, \qquad (9)$$

where V_0 is external electric voltage. Substituting Eq. (9) into Eq. (8) yields

$$E_x = \cos\left(\frac{\pi z}{h}\right) \frac{\partial \phi}{\partial x}, \qquad (10)$$

$$E_\theta = \cos\left(\frac{\pi z}{h}\right) \frac{\partial \phi}{R \partial \theta}, \qquad (11)$$

$$E_z = -\frac{\pi}{h} \sin\left(\frac{\pi z}{h}\right) \phi - \frac{2 V_0}{h}. \qquad (12)$$

Based on Kelvin–Voigt (Ghorbanpour Arani *et al.* 2015c) model, the elastic constant of structurecan be defined as

$$C_{ij}^{(k)} = C_{ij}^{(k)} \left(1 + g \frac{\partial}{\partial t}\right), \qquad (13)$$

where g is structural damping parameter. In the above equations, the effect of viscoelasticity in mechanical form has been considered and electrical Hysteresis effect (Jalili 2010) has been ignored.

4. Motion equations

Here, three theories of CST, FSDT and SSDT are used for mathematical modelling of system.

4.1 CST

Based on CST, the displacement fieldscan be expressed as follows (Amabili 2008)

$$u_1(x, \theta, z, t) = u(x, \theta, t) - z \frac{\partial w(x, \theta, t)}{\partial x}, \qquad (14a)$$

$$u_2(x, \theta, z, t) = v(x, \theta, t) - z \frac{\partial w(x, \theta, t)}{R \partial \theta}, \qquad (14b)$$

$$u_3(x, \theta, z, t) = w(x, \theta, t), \qquad (14c)$$

where $u(x, \theta, t)$, $v(x, \theta, t)$ and $w(x, \theta, t)$ are translations of a point at the middle-surface of the shell. Using Donnell's theory, the nonlinear strain-displacement relations may be expressed as

$$\varepsilon_{xx} = \frac{\partial u}{\partial x} + \frac{1}{2}\left(\frac{\partial w}{\partial x}\right)^2 - z \frac{\partial^2 w}{\partial x^2}, \qquad (15a)$$

$$\varepsilon_{\theta\theta} = \frac{\partial v}{R \partial \theta} + \frac{w}{R} + \frac{1}{2}\left(\frac{\partial w}{R \partial \theta}\right)^2 - z \frac{\partial^2 w}{R^2 \partial \theta^2}, \qquad (15b)$$

$$\gamma_{x\theta} = \frac{\partial u}{R\partial \theta} + \frac{\partial v}{\partial x} + \frac{\partial w}{\partial x}\frac{\partial w}{R\partial \theta} - 2z\frac{\partial^2 w}{R\partial x\partial \theta}. \qquad (15c)$$

The piezoelectric basic equations for CST may be simplified as

$$\begin{bmatrix} \sigma_{xx} \\ \sigma_{\theta\theta} \\ \tau_{x\theta} \end{bmatrix} = \begin{bmatrix} C_{11} & C_{12} & 0 \\ C_{12} & C_{22} & 0 \\ 0 & 0 & C_{66} \end{bmatrix} \begin{Bmatrix} \varepsilon_{xx} \\ \varepsilon_{\theta\theta} \\ \gamma_{x\theta} \end{Bmatrix} - \begin{bmatrix} 0 & 0 & e_{31} \\ 0 & 0 & e_{32} \\ 0 & 0 & 0 \end{bmatrix} \begin{Bmatrix} E_x \\ E_\theta \\ E_z \end{Bmatrix}, \qquad (16)$$

$$\begin{bmatrix} D_x \\ D_\theta \\ D_z \end{bmatrix} = \begin{bmatrix} 0 & 0 & 0 \\ 0 & 0 & 0 \\ e_{31} & e_{32} & 0 \end{bmatrix} \begin{Bmatrix} \varepsilon_{xx} \\ \varepsilon_{\theta\theta} \\ \gamma_{x\theta} \end{Bmatrix} + \begin{bmatrix} \in_{11} & 0 & 0 \\ 0 & \in_{22} & 0 \\ 0 & 0 & \in_{33} \end{bmatrix} \begin{Bmatrix} E_x \\ E_\theta \\ E_z \end{Bmatrix}. \qquad (17)$$

The potential energy of CST can be written as follows

$$U = 0.5\int \Bigg(N_{xx}\left(\frac{\partial u}{\partial x} + \frac{1}{2}\left(\frac{\partial w}{\partial x} \right)^2 \right)$$
$$+ N_{\theta\theta}\left(\frac{\partial v}{R\partial \theta} + \frac{w}{R} + \frac{1}{2}\left(\frac{\partial w}{R\partial \theta} \right)^2 \right)$$
$$+ N_{x\theta}\left(\frac{\partial u}{R\partial \theta} + \frac{\partial v}{\partial x} + \frac{\partial w}{R\partial \theta}\frac{\partial w}{\partial x} \right) - M_{xx}\frac{\partial^2 w}{\partial x^2}$$
$$- M_{\theta\theta}\frac{\partial^2 w}{R^2\partial\theta^2} - 2M_{x\theta}\frac{\partial^2 w}{R\partial\theta\partial x} \Bigg)dA \qquad (18)$$
$$-0.5\int \left(\begin{array}{l} D_x\left(\cos\left(\frac{\pi z}{h} \right)\frac{\partial\phi}{\partial x} \right) + D_\theta\left(\cos\left(\frac{\pi z}{h} \right)\frac{\partial\phi}{R\partial\theta} \right) \\ + D_z\left(-\frac{\pi}{h}\sin\left(\frac{\pi z}{h} \right)\phi - \frac{2V_0}{h} \right) \end{array} \right) dz\,dA.$$

where the stress resultants (N_{xx}, $N_{\theta\theta}$, $N_{x\theta}$, M_{xx}, $M_{\theta\theta}$, $M_{x\theta}$) are defined in Appendix B. The kinetic energy of CST can be expressed as follows

$$K = 0.5\int \Bigg[I_0\left(\left(\frac{\partial u}{\partial t} \right)^2 + \left(\frac{\partial v}{\partial t} \right)^2 + \left(\frac{\partial w}{\partial t} \right)^2 \right)$$
$$-2I_1\left(\frac{\partial u}{\partial t}\frac{\partial^2 w}{\partial t\partial x} + \frac{\partial v}{\partial t}\frac{\partial^2 w}{R\partial t\partial\theta} \right) \qquad (19)$$
$$+ I_2\left(\left(\frac{\partial^2 w}{\partial t\partial x} \right)^2 + \left(\frac{\partial^4 w}{R^2\partial t^2\partial\theta^2} \right)^2 \right) \Bigg]dA.$$

where the moment of inertia (I_0, I_1, I_2) are defined in Appendix B. The external works can be induced by nonlinear orthotropic visco-Pasternak medium, rotating fluid in the separator and 2D magnetic fields due to the existence of SWCNTs. The force induced by nonlinear orthotropic visco-Pasternak foundation can be written as (Ghoorbanpour Arani *et al.* 2015c)

$$q_e = -k_{1w}w - k_{2w}w^3 - c_d\dot{w} \qquad (20)$$

$$+ k_{g\xi}\left(\cos^2\theta\frac{\partial^2 w}{\partial x^2} + 2\cos\theta\sin\theta\frac{\partial^2 w}{\partial x\partial y} + \sin^2\theta\frac{\partial^2 w}{\partial y^2} \right)$$
$$+ k_{g\zeta}\left(\sin^2\theta\frac{\partial^2 w}{\partial x^2} - 2\sin\theta\cos\theta\frac{\partial^2 w}{\partial x\partial y} + \cos^2\theta\frac{\partial^2 w}{\partial y^2} \right), \qquad (20)$$

where angle θ describes the local ξ direction of orthotropic foundation with respect to the global x-axis of the system; k_{1w}, k_{2w}, c_d, $k_{g\xi}$ and $k_{g\zeta}$, respectively are linear spring, nonlinear spring, damper, ξ-shear and ζ-shear constants.

The pressure induced by a fluid (P_{fluid}) can be obtained by the linearized Bernoulli formula as follows (Bochkarev and Matveenko 2013a)

$$P_{Fluid} = \rho\left(\frac{\partial\Phi}{\partial t} + U\frac{\partial\Phi}{\partial x} + \omega_f\frac{\partial\Phi}{\partial\theta} \right) \qquad (21)$$

where ρ, U and ω_f are the density, axial velocity and angular velocity of the fluid. Using Eqs. (A1)-(A6), the generated forces and the bending moment caused by Lorentz force may be calculated as (Ghoorbanpour Arani *et al.* 2015c)

$$R_x^m = \eta h H_\theta^2\delta_{\theta\vartheta}\left(\frac{\partial^2 u}{\partial x^2} + \frac{\partial^2 u}{R^2\partial\theta^2} \right), \qquad (22a)$$

$$R_\theta^m = \eta h H_x^2\delta_{x\vartheta}\left(\frac{\partial^2 v}{\partial x^2} + \frac{\partial^2 v}{R^2\partial\theta^2} \right), \qquad (22b)$$

$$R_z^m = \eta h\left[H_\theta^2\delta_{\theta\vartheta}\left(\frac{\partial^2 w}{R^2\partial\theta^2} - \frac{\partial^2 w}{\partial x^2} \right) \right.$$
$$\left. + H_x^2\delta_{x\vartheta}\left(\frac{\partial^2 w}{\partial x^2} - \frac{\partial^2 w}{R^2\partial\theta^2} \right) \right], \qquad (22c)$$

$$R_z^m = \eta h\left[H_\theta^2\delta_{\theta\vartheta}\left(\frac{\partial^2 w}{R^2\partial\theta^2} - \frac{\partial^2 w}{\partial x^2} \right) \right.$$
$$\left. + H_x^2\delta_{x\vartheta}\left(\frac{\partial^2 w}{\partial x^2} - \frac{\partial^2 w}{R^2\partial\theta^2} \right) \right], \qquad (23a)$$

$$M_\theta^m = -\frac{\eta h^3 H_x^2}{12}\delta_{x\vartheta}\left(\frac{\partial^3 w}{R^3\partial\theta^3} + \frac{\partial^3 w}{R\partial\theta\partial x^2} \right). \qquad (23b)$$

The motion equations can be derived based on Hamilton's principle as follows

$$\int_0^t (\delta U - \delta W - \delta K)dt = 0. \qquad (24)$$

Substituting Eqs. (18)-(23) into Eq. (24) yields the CST motion equations as follows

$$\delta u: \quad \frac{\partial N_{xx}}{\partial x} + \frac{\partial N_{x\theta}}{R\partial\theta} + R_x^m = I_0\frac{\partial^2 u}{\partial t^2}, \qquad (25)$$

$$\delta v: \quad \frac{\partial N_{x\theta}}{\partial x} + \frac{\partial N_{\theta\theta}}{R\partial\theta} + R_\theta^m = I_0\frac{\partial^2 v}{\partial t^2}, \qquad (26)$$

$$\delta w: \quad \frac{\partial^2 M_{xx}}{\partial x^2} + \frac{\partial^2 M_{\theta\theta}}{R^2 \partial \theta^2} + 2\frac{\partial^2 M_{x\theta}}{R\partial x\partial \theta}$$

$$-\frac{N_\theta}{R} + \frac{\partial}{\partial x}\left(N_x^f \frac{\partial w}{\partial x}\right) + \frac{\partial}{R\partial\theta}\left(N_\theta^f \frac{\partial w}{R\partial\theta}\right) \qquad (27)$$

$$+ q_e + q_f + \overline{R}_Z^m + M_x^m + M_\theta^m = I_0 \frac{\partial^2 w}{\partial t^2},$$

$$\delta\phi: \quad G_X + G_\theta - G_Z = 0. \qquad (28)$$

$$\delta\Phi: \quad \frac{\partial^2 \Phi}{\partial x^2} + \frac{1}{R^2}\frac{\partial^2 \Phi}{\partial \theta^2}$$

$$-\frac{1}{C^2}\left(\frac{\partial^2 \Phi}{\partial t^2} + U^2\frac{\partial^2 \Phi}{\partial x^2} + 2U\frac{\partial^2 \Phi}{\partial x\partial t}\right)$$

$$= \frac{2\omega_f}{C}\left(M\frac{\partial^2 \Phi}{\partial x\partial\theta} + \frac{1}{C}\frac{\partial^2 \Phi}{\partial\theta\partial t}\right) \qquad (29)$$

$$+ \frac{\omega_f^2}{C^2}\left(\frac{\partial^2 \Phi}{\partial\theta^2} - R\left(\frac{\partial w}{\partial t} + U\frac{\partial w}{\partial x} + \omega_f \frac{\partial w}{\partial\theta}\right)\right)$$

Noted that the last equation is the perturbation velocity potential Φ, in the cylindrical coordinate system (x, θ, z) for small perturbations to describe the motion of the rotating fluid. In addition, C and $M = U/C$ are respectively sound velocity in liquid-particle and the Mach number.

In above relations N_x^f and N_θ^f are combination of mechanical and electrical forces which can be expressed in dimensionless form as

$$N_x^f = N_x^M + N_x^E \rightarrow \begin{cases} N_x^M = 0, \\ N_x^E = 2e_{31}V_0, \end{cases} \qquad (30a)$$

$$N_\theta^f = N_\theta^M + N_\theta^E \rightarrow \begin{cases} N_\theta^M = 0, \\ N_\theta^E = 2e_{32}V_0, \end{cases} \qquad (30b)$$

The following boundary conditions are assumed for the separator based on CST

• **Simple-Simple (SS)**

$$x = 0 \Rightarrow v = w = M_{xx} = \phi = \Phi = 0,$$

$$x = L \Rightarrow v = w = M_{xx} = \phi = \frac{\partial\Phi}{\partial x} = 0, \qquad (31a)$$

• **Clamped- Clamped (CC)**

$$x = 0 \Rightarrow u = v = w = \phi = \Phi = 0,$$

$$x = 0 \Rightarrow u = v = w = \phi = \frac{\partial\Phi}{\partial x} = 0, \qquad (31b)$$

• **Clamped- Simple (CS)**

$$x = 0 \Rightarrow u = v = w = \phi = \Phi = 0,$$

$$x = L \Rightarrow v = w = M_{xx} = \phi = \frac{\partial\Phi}{\partial x} = 0. \qquad (31c)$$

4.2 FSDT

Based on FSDT, the displacement field can be expressed as may be written as (Amabili 2008)

$$u_1(x,\theta,z,t) = u(x,\theta,t) + z\psi_x(x,\theta,t), \qquad (32a)$$

$$u_2(x,\theta,z,t) = v(x,\theta,t) + z\psi_\theta(x,\theta,t), \qquad (32b)$$

$$u_3(x,\theta,z,t) = w(x,\theta,t), \qquad (32c)$$

where $\psi_x(x, \theta, t)$ and $\psi_\theta(x, \theta, t)$ are the rotations of the normal to the mid-plane about x- and θ- directions, respectively. However, the nonlinear strain-displacement relations associated with the above displacement field can be derived as

$$\varepsilon_{xx} = \frac{\partial u}{\partial x} + \frac{1}{2}\left(\frac{\partial w}{\partial x}\right)^2 + z\frac{\partial\psi_x}{\partial x}, \qquad (33a)$$

$$\varepsilon_{\theta\theta} = \frac{\partial v}{R\partial\theta} + \frac{w}{R} + \frac{1}{2}\left(\frac{\partial w}{R\partial\theta}\right)^2 + z\frac{\partial\psi_\theta}{R\partial\theta}, \qquad (33b)$$

$$\gamma_{\theta z} = \frac{\partial w}{R\partial\theta} - \frac{v}{R} + \psi_\theta, \qquad (33c)$$

$$\gamma_{xz} = \frac{\partial w}{\partial x} + \psi_x, \qquad (33d)$$

$$\gamma_{x\theta} = \frac{\partial v}{\partial x} + \frac{\partial u}{R\partial\theta} + \frac{\partial w}{\partial x}\frac{\partial w}{R\partial\theta} + z\left(\frac{\partial\psi_x}{R\partial\theta} + \frac{\partial\psi_\theta}{\partial x}\right). \qquad (33e)$$

Eqs. (6) and (7) for FSDT can be simplified as

$$\begin{bmatrix} \sigma_{xx} \\ \sigma_{\theta\theta} \\ \tau_{\theta z} \\ \tau_{xz} \\ \tau_{x\theta} \end{bmatrix} = \begin{bmatrix} C_{11} & C_{12} & 0 & 0 & 0 \\ C_{12} & C_{22} & 0 & 0 & 0 \\ 0 & 0 & C_{44} & 0 & 0 \\ 0 & 0 & 0 & C_{55} & 0 \\ 0 & 0 & 0 & 0 & C_{66} \end{bmatrix}\begin{bmatrix} \varepsilon_{xx} \\ \varepsilon_{\theta\theta} \\ \gamma_{\theta z} \\ \gamma_{xz} \\ \gamma_{x\theta} \end{bmatrix}$$

$$-\begin{bmatrix} 0 & 0 & e_{31} \\ 0 & 0 & e_{32} \\ 0 & e_{24} & 0 \\ e_{15} & 0 & 0 \\ 0 & 0 & 0 \end{bmatrix}\begin{Bmatrix} E_x \\ E_\theta \\ E_z \end{Bmatrix}, \qquad (34a)$$

$$\begin{bmatrix} D_x \\ D_\theta \\ D_z \end{bmatrix} = \begin{bmatrix} 0 & 0 & 0 & e_{15} & 0 \\ 0 & 0 & e_{24} & 0 & 0 \\ e_{31} & e_{32} & 0 & 0 & 0 \end{bmatrix}\begin{Bmatrix} \varepsilon_{xx} \\ \varepsilon_{\theta\theta} \\ \gamma_{\theta z} \\ \gamma_{xz} \\ \gamma_{x\theta} \end{Bmatrix} + \begin{bmatrix} \in_{11} & 0 & 0 \\ 0 & \in_{22} & 0 \\ 0 & 0 & \in_{33} \end{bmatrix}\begin{Bmatrix} E_x \\ E_\theta \\ E_z \end{Bmatrix}. \qquad (34b)$$

The potential energy of FSDT can be written as follows

$$U = 0.5 \int \left(N_{xx} \left(\frac{\partial u}{\partial x} + \frac{1}{2} \left(\frac{\partial w}{\partial x} \right)^2 \right) \right.$$

$$+ N_{\theta\theta} \left(\frac{\partial v}{R\partial\theta} + \frac{w}{R} + \frac{1}{2} \left(\frac{\partial w}{R\partial\theta} \right)^2 \right)$$

$$+ Q_\theta \left(\frac{\partial w}{R\partial\theta} - \frac{v}{R} + \psi_\theta \right) + Q_x \left(\frac{\partial w}{\partial x} + \psi_x \right)$$

$$+ N_{x\theta} \left(\frac{\partial v}{\partial x} + \frac{\partial u}{R\partial\theta} + \frac{\partial w}{\partial x} \frac{\partial w}{R\partial\theta} \right) + M_{xx} \frac{\partial \psi_x}{\partial x} \qquad (35)$$

$$+ M_{\theta\theta} \frac{\partial \psi_\theta}{R\partial\theta} + M_{x\theta} \left(\frac{\partial \psi_x}{R\partial\theta} + \frac{\partial \psi_\theta}{\partial x} \right) \right) dA$$

$$- 0.5 \int \left(D_x \left(\cos\left(\frac{\pi z}{h} \right) \frac{\partial \phi}{\partial x} \right) + D_\theta \left(\cos\left(\frac{\pi z}{h} \right) \frac{\partial \phi}{R\partial\theta} \right) \right.$$

$$+ \left. D_z \left(-\frac{\pi}{h} \sin\left(\frac{\pi z}{h} \right) \phi - \frac{2V_0}{h} \right) \right) dz dA.$$

where the stress resultants (N_{xx}, $N_{\theta\theta}$, $N_{x\theta}$, Q_x, Q_θ, M_{xx}, $M_{\theta\theta}$, $M_{x\theta}$) are defined in Appendix B. The kinetic energy of FSDT can be obtained as follows

$$K = 0.5 \int \left[I_0 \left(\left(\frac{\partial u}{\partial t} \right)^2 + \left(\frac{\partial v}{\partial t} \right)^2 + \left(\frac{\partial w}{\partial t} \right)^2 \right) \right.$$

$$+ 2I_1 \left(\frac{\partial u}{\partial t} \frac{\partial \psi_x}{\partial t} + \frac{\partial v}{\partial t} \frac{\partial \psi_\theta}{\partial t} \right) \qquad (36)$$

$$+ \left. I_2 \left(\left(\frac{\partial \psi_x}{\partial t} \right)^2 + \left(\frac{\partial \psi_\theta}{\partial t} \right)^2 \right) \right] dA.$$

where the moment of inertia (I_0, I_1, I_2) are defined in Appendix B. However, Eqs. (A1)-(A3) and (A7)-(A9), the generated forces and the bending moment caused by Lorentz force may be calculated by

$$R_x^m = \eta h H_\theta^2 \delta_{\theta\vartheta} \left(\frac{\partial^2 u}{\partial x^2} + \frac{\partial^2 u}{R^2 \partial \theta^2} \right), \qquad (37a)$$

$$R_\theta^m = \eta h H_x^2 \delta_{x\vartheta} \left(\frac{\partial^2 v}{\partial x^2} + \frac{\partial^2 v}{R^2 \partial \theta^2} \right), \qquad (37b)$$

$$R_z^m = \eta h \left[H_\theta^2 \delta_{\theta\vartheta} \left(\frac{\partial^2 w}{\partial x^2} + \frac{\partial \psi_\theta}{R\partial\theta} \right) \right.$$

$$+ \left. H_x^2 \delta_{x\vartheta} \left(\frac{\partial^2 w}{\partial x^2} + \frac{\partial \psi_\theta}{R\partial\theta} \right) \right], \qquad (37c)$$

$$M_x^m = \frac{\eta h^3 H_\theta^2}{12} \delta_{\theta\vartheta} \left(\frac{\partial^2 \psi_x}{\partial x^2} + \frac{\partial^2 \psi_x}{R^2 \partial \theta^2} \right), \qquad (38a)$$

$$M_\theta^m = \frac{\eta h^3 H_x^2}{12} \delta_{x\vartheta} \left(\frac{\partial^2 \psi_\theta}{R^2 \partial \theta^2} + \frac{\partial^2 \psi_\theta}{\partial x^2} \right). \qquad (38b)$$

Noted that the induced forces due to the viscoelastic foundation and rotating fluid are the same as Eqs. (20) and (21), respectively. Substituting Eqs. (35), (36), (37), (38), (20) and (21) into Eq. (24) yields the CST motion equations as follows

$$\delta u: \quad \frac{\partial N_{xx}}{\partial x} + \frac{\partial N_{x\theta}}{R\partial\theta} + R_x^m = I_0 \frac{\partial^2 u}{\partial t^2} + I_1 \frac{\partial^2 \psi_x}{\partial t^2}, \qquad (39)$$

$$\delta v: \quad \frac{\partial N_{x\theta}}{\partial x} + \frac{\partial N_{\theta\theta}}{R\partial\theta} + \frac{Q_\theta}{R} + R_\theta^m = I_0 \frac{\partial^2 v}{\partial t^2} + I_1 \frac{\partial^2 \psi_\theta}{\partial t^2}, \qquad (40)$$

$$\delta w: \quad \frac{\partial Q_x}{\partial x} + \frac{\partial Q_\theta}{R\partial\theta} + \frac{\partial}{\partial x} \left(N_x^f \frac{\partial w}{\partial x} \right) + \frac{\partial}{R\partial\theta} \left(N_\theta^f \frac{\partial w}{R\partial\theta} \right)$$

$$+ q_e + q_f + R_Z^m = I_0 \frac{\partial^2 w}{\partial t^2}, \qquad (41)$$

$$\delta \psi_X: \quad \frac{\partial M_{xx}}{\partial x} + \frac{\partial M_{x\theta}}{R\partial\theta} - Q_x + M_x^m$$

$$= I_1 \frac{\partial^2 u}{\partial t^2} + I_2 \frac{\partial^2 \psi_X}{\partial t^2}, \qquad (42)$$

$$\delta \psi_\theta: \quad \frac{\partial M_{x\theta}}{\partial x} + \frac{\partial M_{\theta\theta}}{R\partial\theta} - Q_\theta + M_\theta^m$$

$$= I_1 \frac{\partial^2 v}{\partial t^2} + I_2 \frac{\partial^2 \psi_\theta}{\partial t^2}, \qquad (43)$$

$$\delta \phi: \quad G_X + G_\theta - G_Z = 0. \qquad (44)$$

$$\delta \Phi: \quad \frac{\partial^2 \Phi}{\partial x^2} + \frac{1}{R^2} \frac{\partial^2 \Phi}{\partial \theta^2}$$

$$- \frac{1}{C_{eff}^2} \left(\frac{\partial^2 \Phi}{\partial t^2} + U^2 \frac{\partial^2 \Phi}{\partial x^2} + 2U \frac{\partial^2 \Phi}{\partial x \partial t} \right)$$

$$= \frac{2\Omega_f}{C_{eff}} \left(M \frac{\partial^2 \Phi}{\partial x \partial \theta} + \frac{1}{C} \frac{\partial^2 \Phi}{\partial \theta \partial t} \right) \qquad (45)$$

$$+ \frac{\Omega_f^2}{C_{eff}^2} \left(\frac{\partial^2 \Phi}{\partial \theta^2} - R \left(\frac{\partial w}{\partial t} + U \frac{\partial w}{\partial x} + \Omega_f \frac{\partial w}{\partial \theta} \right) \right)$$

The following boundary conditions are assumed for the separator based on FSDT:

• **Simple-Simple (SS)**

$$x = 0 \Rightarrow v = w = \psi_\theta = N_{xx} = M_{xx} = \phi = \Phi = 0,$$

$$x = L \Rightarrow v = w = \psi_\theta = N_{xx} = M_{xx} = \phi = \frac{\partial \Phi}{\partial x} = 0, \qquad (46a)$$

• **Clamped- Clamped (CC)**

$$x = 0 \Rightarrow u = v = w = \psi_x = \psi_\theta = \phi = \Phi = 0,$$

$$x = 0 \Rightarrow u = v = w = \psi_x = \psi_\theta = \phi = \frac{\partial \Phi}{\partial x} = 0, \qquad (46b)$$

• **Clamped- Simple (CS)**

$$x = 0 \Rightarrow u = v = w = \psi_x = \psi_\theta = \phi = \Phi = 0,$$

$$x = L \Rightarrow v = w = \psi_x = N_{xx} = M_{xx} = \phi = \frac{\partial \Phi}{\partial x} = 0. \quad (46c)$$

4.3 SSDT

Based on SSDT, the displacement field can be obtained as (Thai and Vo 2013)

$$u_1(x,\theta,z,t) = u(x,\theta,t) - z\frac{\partial w_b(x,\theta,t)}{\partial x} - f\frac{\partial w_s(x,\theta,t)}{\partial x}, \quad (47a)$$

$$u_2(x,\theta,z,t) = v(x,\theta,t) - z\frac{\partial w_b(x,\theta,t)}{R\partial \theta} - f\frac{\partial w_s(x,\theta,t)}{R\partial \theta}, \quad (47b)$$

$$u_3(x,\theta,z,t) = w_b(x,\theta,t) + w_s(x,\theta,t), \quad (47c)$$

where $f = z - \frac{h}{\pi}\sin\frac{\pi z}{h}$; $w_b(x, \theta, t)$ and $w_s(x, \theta, t)$ are the bending and shear components of transverse displacement. The nonlinear kinematic relations can be expressed as follows

$$\varepsilon_{xx} = \frac{\partial u}{\partial x} + \frac{1}{2}\left(\frac{\partial w_b}{\partial x}\right)^2 + \frac{1}{2}\left(\frac{\partial w_s}{\partial x}\right)^2 - z\frac{\partial^2 w_b}{\partial x^2} - f\frac{\partial^2 w_s}{\partial x^2}, \quad (48a)$$

$$\varepsilon_{\theta\theta} = \frac{\partial v}{R\partial \theta} + \frac{w_b}{R} + \frac{w_s}{R} + \frac{1}{2}\left(\frac{\partial w_b}{R\partial \theta}\right)^2 + \frac{1}{2}\left(\frac{\partial w_s}{R\partial \theta}\right)^2$$
$$+ \frac{1}{2}\left(\frac{\partial w_s}{R\partial \theta}\right)^2 - z\frac{\partial^2 w_b}{R^2\partial \theta^2} - f\frac{\partial^2 w_b}{R^2\partial \theta^2}, \quad (48b)$$

$$\gamma_{\theta z} = p\frac{\partial w_s}{R\partial \theta} - \frac{v}{R}, \quad (48c)$$

$$\gamma_{xz} = p\frac{\partial w_s}{\partial x}, \quad (48d)$$

$$\gamma_{x\theta} = \frac{\partial u}{R\partial \theta} + \frac{\partial v}{\partial x} + \left(\frac{\partial w_b}{\partial x} + \frac{\partial w_s}{\partial x}\right)\left(\frac{\partial w_b}{R\partial \theta} + \frac{\partial w_s}{R\partial \theta}\right).$$
$$- 2z\frac{\partial^2 w_b}{R\partial x\partial \theta} - 2f\frac{\partial^2 w_s}{R\partial x\partial \theta}, \quad (48e)$$

where $p = \cos\frac{\pi z}{h}$. Eqs. (6) and (7) for SSDT can be simplified as

$$\begin{bmatrix} \sigma_{xx} \\ \sigma_{\theta\theta} \\ \tau_{\theta z} \\ \tau_{xz} \\ \tau_{x\theta} \end{bmatrix} = \begin{bmatrix} C_{11} & C_{12} & 0 & 0 & 0 \\ C_{12} & C_{22} & 0 & 0 & 0 \\ 0 & 0 & C_{44} & 0 & 0 \\ 0 & 0 & 0 & C_{55} & 0 \\ 0 & 0 & 0 & 0 & C_{66} \end{bmatrix} \begin{bmatrix} \varepsilon_{xx} \\ \varepsilon_{\theta\theta} \\ \gamma_{\theta z} \\ \gamma_{xz} \\ \gamma_{x\theta} \end{bmatrix} \quad (49a)$$

$$- \begin{bmatrix} 0 & 0 & e_{31} \\ 0 & 0 & e_{32} \\ 0 & e_{24} & 0 \\ e_{15} & 0 & 0 \\ 0 & 0 & 0 \end{bmatrix} \begin{bmatrix} E_x \\ E_\theta \\ E_z \end{bmatrix}, \quad (49a)$$

$$\begin{bmatrix} D_x \\ D_\theta \\ D_z \end{bmatrix} = \begin{bmatrix} 0 & 0 & 0 & e_{15} & 0 \\ 0 & 0 & e_{24} & 0 & 0 \\ e_{31} & e_{32} & 0 & 0 & 0 \end{bmatrix} \begin{Bmatrix} \varepsilon_{xx} \\ \varepsilon_{\theta\theta} \\ \gamma_{\theta z} \\ \gamma_{xz} \\ \gamma_{x\theta} \end{Bmatrix} \begin{bmatrix} \in_{11} & 0 & 0 \\ 0 & \in_{22} & 0 \\ 0 & 0 & \in_{33} \end{bmatrix} \begin{Bmatrix} E_x \\ E_\theta \\ E_z \end{Bmatrix}. \quad (49b)$$

The potential energy of SSDT can be expressed as follows

$$U = 0.5\int_A\left(N_{xx}\left(\frac{\partial u}{\partial x} + \frac{1}{2}\left(\frac{\partial w_b}{\partial x}\right)^2 + \frac{1}{2}\left(\frac{\partial w_s}{\partial x}\right)^2\right)\right.$$
$$+ N_{\theta\theta}\left(\frac{\partial v}{R\partial \theta} + \frac{w_b}{R} + \frac{w_s}{R} + \frac{1}{2}\left(\frac{\partial w_b}{R\partial \theta}\right)^2 + \frac{1}{2}\left(\frac{\partial w_s}{\partial x}\right)^2\right)$$
$$+ N_{x\theta}\left(\frac{\partial v}{\partial x} + \frac{\partial u}{R\partial \theta} + \left(\frac{\partial w_b}{Rx} + \frac{\partial w_s}{\partial x}\right)\left(\frac{\partial w_b}{R\partial \theta} + \frac{\partial w_s}{R\partial \theta}\right)\right)$$
$$- Q_\theta\frac{v}{R} - M_{xx}\left(\frac{\partial^2 w_b}{Rx^2}\right) - M_{\theta\theta}\left(\frac{\partial^2 w_b}{R^2\partial \theta^2}\right)$$
$$- 2M_{2\theta}\left(\frac{\partial^2 w_b}{R\partial \theta Rx}\right) + S_{xx}\frac{\partial^2 w_s}{Rx^2} - S_{\theta\theta}\frac{\partial^2 w_s}{R^2\partial \theta^2}$$
$$- 2S_{2\theta}\frac{\partial^2 w_s}{R\partial \theta Rx} + F_{\theta\theta}\frac{\partial w_s}{R\partial \theta} + F_{xx}\frac{\partial w_s}{\partial x}\right)dA$$
$$- 0.5\int\left(D_x\left(\cos\left(\frac{\pi z}{h}\right)\frac{\partial \phi}{\partial x}\right) + D_\theta\left(\cos\left(\frac{\pi z}{h}\right)\frac{\partial \phi}{R\partial \theta}\right)\right.$$
$$\left.+ D_z\left(-\frac{\pi}{h}\sin\left(\frac{\pi z}{h}\right)\varphi - \frac{2V_0}{h}\right)\right)dzdA. \quad (50)$$

where the stress resultants (N_{xx}, $N_{\theta\theta}$, $N_{x\theta}$, Q_x, Q_θ, M_{xx}, $M_{\theta\theta}$, $M_{x\theta}$, S_{xx}, $S_{\theta\theta}$, $S_{x\theta}$, F_{xx}, $F_{\theta\theta}$) are defined in Appendix B. The kinetic energy of SSDT can be obtained as follows

$$K = 0.5\int\left(I_0\left(\left(\frac{\partial u}{\partial t}\right)^2 + \left(\frac{\partial v}{\partial t}\right)^2 + \left(\frac{\partial w_b}{\partial t}\right)^2 + \left(\frac{\partial w_s}{\partial t}\right)^2\right.\right.$$
$$\left.+ 2\frac{\partial w_b}{\partial t}\frac{\partial w_s}{\partial t}\right) - 2I_1\left(\frac{\partial u}{\partial t}\frac{\partial^2 w_b}{\partial t\partial x} + \frac{\partial v}{\partial t}\frac{\partial^2 w_b}{R\partial t\partial \theta}\right)$$
$$+ I_2\left(\left(\frac{\partial^2 w_b}{\partial t\partial x}\right)^2 + \left(\frac{\partial^2 w_b}{R\partial t\partial \theta}\right)^2\right)$$
$$+ I_3\left(\left(\frac{\partial^2 w_s}{\partial t\partial x}\right)^2 + \left(\frac{\partial^2 w_s}{R\partial t\partial \theta}\right)^2\right) \quad (51)$$

$$+2I_4\left(\frac{\partial^2 w_b}{\partial t\partial x}\frac{\partial^2 w_s}{\partial t\partial x}+\frac{\partial^2 w_b}{R\partial t\partial\theta}\frac{\partial^2 w_s}{R\partial t\partial\theta}\right)$$
$$+2I_5\left(\frac{\partial u}{\partial t}\frac{\partial^2 w_s}{\partial t\partial x}+\frac{\partial v}{\partial t}\frac{\partial^2 w_s}{R\partial t\partial\theta}\right)\Bigg)dA. \tag{51}$$

where the moment of inertia (I_0, I_1, I_2, I_3, I_4, I_5) are defined in Appendix B. However, using Eqs. (A1)-(A3) and (A10)-(A12), the generated forces and the bending moment caused by Lorentz force may be calculated by

$$R_x^m=\eta h H_\theta^2\delta_{\theta\vartheta}\left(\frac{\partial^2 u}{\partial x^2}+\frac{\partial^2 u}{R^2\partial\theta^2}\right), \tag{52a}$$

$$R_\theta^m=\eta h H_x^2\delta_{x\vartheta}\left(\frac{\partial^2 v}{\partial x^2}+\frac{\partial^2 v}{R^2\partial\theta^2}\right), \tag{52b}$$

$$R_z^m=\eta h\Bigg[H_\theta^2\delta_{\theta\vartheta}\left(\frac{\partial^2 w_b}{R^2\partial\theta^2}+\frac{\partial^2 w_s}{R^2\partial\theta^2}-\frac{\partial^2 w_b}{\partial x^2}\right)$$
$$-\left(1-\frac{2}{\pi}\right)\frac{\partial^2 w_s}{\partial x^2}+H_x^2\delta_{x\vartheta}\left(\frac{\partial^2 w_b}{\partial x^2}+\frac{\partial^2 w_s}{\partial x^2}\right) \tag{52c}$$
$$-\frac{\partial^2 w_b}{R^2\partial\theta^2}-\left(1-\frac{2}{\pi}\right)\frac{\partial^2 w_s}{R^2\partial\theta^2}\right)\Bigg],$$

$$M_x^m$$
$$=-\frac{\eta h^3 H_\theta^2}{12}\delta_{\theta\vartheta}\left(\frac{\partial^3 w_b}{\partial x^3}+\frac{\partial^3 w_b}{R^2\partial x\partial\theta^2}+\frac{\partial^3 w_s}{\partial x^3}+\frac{\partial^3 w_s}{R^2\partial x\partial\theta^2}\right)$$
$$+\frac{2\eta h^3 H_\theta^2}{\pi^3}\delta_{\theta\vartheta}\left(\frac{\partial^3 w_s}{\partial x^3}+\frac{\partial^3 w_s}{R^2\partial x\partial\theta^2}\right), \tag{53a}$$

$$M_\theta^m$$
$$=-\frac{\eta h^3 H_x^2}{12}\delta_{x\vartheta}\left(\frac{\partial^3 w_b}{R^3\partial\theta^3}+\frac{\partial^3 w_b}{R\partial\theta\partial x^2}+\frac{\partial^3 w_s}{R^3\partial\theta^3}+\frac{\partial^3 w_s}{R\partial\theta\partial x^2}\right)$$
$$+\frac{2\eta h^3 H_\theta^2}{\pi^3}\delta_{x\vartheta}\left(\frac{\partial^3 w_s}{R^3\partial\theta^3}+\frac{\partial^3 w_s}{R\partial\theta\partial x^2}\right). \tag{53b}$$

Noted that the induced forces due to the viscoelastic foundation and pulsating fluid are the same as Eqs. (20) and (21), respectively. Substituting Eqs. (50)-(53) and (20)-(21) into Eq. (24) yields the SSDT motion equations as follows

$$\delta u:\quad \frac{\partial N_{xx}}{\partial x}+\frac{\partial N_{x\theta}}{R\partial\theta}+R_x^m=I_0\frac{\partial^2 u}{\partial t^2}, \tag{54}$$

$$\delta v:\quad \frac{\partial N_{x\theta}}{\partial x}+\frac{\partial N_{\theta\theta}}{R\partial\theta}+\frac{Q_\theta}{R}+R_\theta^m=I_0\frac{\partial^2 v}{\partial t^2}, \tag{55}$$

$$\delta w_b:\quad \frac{\partial^2 M_{xx}}{\partial x^2}+\frac{\partial^2 M_{\theta\theta}}{R^2\partial\theta^2}+2\frac{\partial^2 M_{x\theta}}{R\partial x\partial\theta}$$
$$-\frac{N_\theta}{R}+\frac{\partial}{\partial x}\left(N_x^f\frac{\partial w_b}{\partial x}\right)+\frac{\partial}{R\partial\theta}\left(N_\theta^f\frac{\partial w_b}{R\partial\theta}\right) \tag{56}$$

$$+q_e+q_f+R_z^m+M_x^m+M_\theta^m$$
$$=I_0\left(\frac{\partial^2 w_b}{\partial t^2}+\frac{\partial^2 w_s}{\partial t^2}\right) \tag{56}$$
$$-(I_2+I_4)\left(\frac{\partial^4 w_b}{\partial t^2\partial x^2}+\frac{\partial^4 w_b}{R^2\partial t^2\partial\theta^2}\right),$$

$$\delta w_s:\quad \frac{\partial^2 S_{xx}}{\partial x^2}+\frac{\partial^2 S_{\theta\theta}}{R^2\partial\theta^2}+2\frac{\partial^2 S_{x\theta}}{R\partial x\partial\theta}+\frac{\partial F_{xx}}{\partial x}+\frac{\partial F_{\theta\theta}}{R\partial\theta}$$
$$+\frac{\partial}{\partial x}\left(N_x^f\frac{\partial w_s}{\partial x}\right)+\frac{\partial}{R\partial\theta}\left(N_\theta^f\frac{\partial w_s}{R\partial\theta}\right)$$
$$+q_e+q_f+R_z^m+M_x^m+M_\theta^m \tag{57}$$
$$=I_0\left(\frac{\partial^2 w_b}{\partial t^2}+\frac{\partial^2 w_s}{\partial t^2}\right)$$
$$-(I_3+I_4)\left(\frac{\partial^4 w_s}{\partial t^2\partial x^2}+\frac{\partial^4 w_s}{R^2\partial t^2\partial\theta^2}\right),$$

$$\delta\phi:\quad G_X+G_\theta-G_Z=0, \tag{58}$$

$$\delta\Phi:\quad \frac{\partial^2\Phi}{\partial x^2}+\frac{1}{R^2}\frac{\partial^2\Phi}{\partial\theta^2}$$
$$-\frac{1}{C_{eff}^2}\left(\frac{\partial^2\Phi}{\partial t^2}+U^2\frac{\partial^2\Phi}{\partial x^2}+2U\frac{\partial^2\Phi}{\partial x\partial t}\right)$$
$$=\frac{2\Omega_f}{C_{eff}}\left(M\frac{\partial^2\Phi}{\partial x\partial\theta}+\frac{1}{C}\frac{\partial^2\Phi}{\partial\theta\partial t}\right) \tag{59}$$
$$+\frac{\Omega_f^2}{C_{eff}^2}\left(\frac{\partial^2\Phi}{\partial\theta^2}-R\left(\frac{\partial w}{\partial t}+U\frac{\partial w}{\partial x}+\Omega_f\frac{\partial w}{\partial\theta}\right)\right)$$

The following boundary conditions are assumed for the separator based on SSDT:

• **Simple-Simple (SS)**

$$x=0\Rightarrow v=w_b=w_s=M_{xx}=\phi=\Phi=0,$$
$$x=L\Rightarrow v=w_b=w_s=M_x=\phi=\frac{\partial\Phi}{\partial x}=0, \tag{60a}$$

• **Clamped- Clamped (CC)**

$$x=0\Rightarrow u=v=w_b=w_s=\phi=\Phi=0,$$
$$x=0\Rightarrow u=v=w_b=w_s=\phi=\frac{\partial\Phi}{\partial x}=0, \tag{60b}$$

• **Clamped- Simple (CS)**

$$x=0\Rightarrow v=w_b=w_s=\phi=\Phi=0,$$
$$x=L\Rightarrow v=w_b=w_s=M_{xx}=\phi=\frac{\partial\Phi}{\partial x}=0. \tag{60c}$$

5. Solution method

There is a lot of numerical method to solve the initial-

and/or boundary value problems which occur in engineering domain. Some of the common numerical methods are FEM, Galerkin method, finite difference method (FDM), GDQM and etc. FEM and FDM for higher-order modes require to a great number of grid points. Therefore these solution methods for all these points need to more CPU time, while the GDQM has several benefits that are listed as below (Bert and Malik 1996, Liew and Liu 2000, Gupta *et al.* 2006)

  (1)   GDQM is a powerful method which can be used to solve numerical problems in the analysis of structural and dynamical systems.

  (2)   The accuracy and convergence of the GDQM is higher than FEM.

  (3)   GDQM is an accurate method for solution of nonlinear differential equations in approximation of the derivatives.

  (4)   This method can easily and exactly satisfy a variety of boundary conditions and require much less formulation and programming effort.

  (5)   Recently, GDQM has been extended to handle irregular shaped.

Due to the above striking merits of the GDQM, in recent years the method has become increasingly popular in the numerical solution of problems in engineering and physical science. DQM is used in this paper which approximates the partial derivative of a function with respect to a spatial variable at a given discrete. Hence, the nth-order and m^{th}-order of partial derivative of function $F(x, \theta)$ with respect to x and θ respectively, can be written at the point (x_i, θ_i), as follows (Nie and Zhong 2007, 2010, Tornabene and Ceruti 2013, Fantuzzi *et al.* 2015, Ghorbanpour Arani *et al.* 2013, 2015c)

$$\frac{d^n F(x_i, \theta_j)}{dx^n} = \sum_{k=1}^{N_x} A_{ik}^{(n)} F(x_k, \theta_j) \qquad n = 1, ..., N_x - 1, \quad (61)$$

$$\frac{d^m F(x_i, \theta_j)}{d\theta^m} = \sum_{l=1}^{N_\theta} B_{jl}^{(m)} F(x_i, \theta_l) \qquad m = 1, ..., N_\theta - 1, \quad (62)$$

$$\frac{d^{n+m} F(x_i, \theta_j)}{dx^n d\theta^m} = \sum_{k=1}^{N_x} \sum_{l=1}^{N_\theta} A_{ik}^{(n)} B_{jl}^{(m)} F(x_k, \theta_l), \quad (63)$$

where $A_{ik}^{(n)}$ and $B_{jl}^{(m)}$ are the weighting coefficients corresponding to the nth-order and m^{th}-order partial derivative of $F(x, \theta)$ with respect to x and θ respectively, which can be written for fist derivative as follows

$$A_{ij}^{(1)} = \begin{cases} \dfrac{M(x_i)}{(x_i - x_j) M(x_j)}, & \text{for} \quad i \neq j, \quad i, j = 1, 2, ..., N_x \\[2em] -\sum_{\substack{j=1 \\ i \neq j}}^{N_x} A_{ij}^{(1)}, & \text{for} \quad i = j, \quad i, j = 1, 2, ..., N_x \end{cases} \quad (64)$$

$$B_{ij}^{(1)} = \begin{cases} \dfrac{P(\theta_i)}{(\theta_i - \theta_j) P(\theta_j)}, & \text{for} \quad i \neq j, \quad i, j = 1, 2, ..., N_\theta \\[2em] -\sum_{\substack{j=1 \\ i \neq j}}^{N_\theta} B_{ij}^{(1)}, & \text{for} \quad i = j, \quad i, j = 1, 2, ..., N_\theta \end{cases} \quad (65)$$

where

$$M(x_i) = \prod_{\substack{j=1 \\ j \neq i}}^{N_x} (x_i - x_j), \quad (66)$$

$$P(\theta_i) = \prod_{\substack{j=1 \\ j \neq i}}^{N_\theta} (\theta_i - \theta_j). \quad (67)$$

Noted that for higher order derivative, the following formulas can be used

$$A_{ij}^{(n)} = n \left(A_{ii}^{(n-1)} A_{ij}^{(1)} - \frac{A_{ij}^{(n-1)}}{(x_i - x_j)} \right), \quad (68)$$

$$B_{ij}^{(m)} = m \left(B_{ii}^{(m-1)} B_{ij}^{(1)} - \frac{B_{ij}^{(m-1)}}{(\theta_i - \theta_j)} \right). \quad (69)$$

In addition, N_θ and N_θ are the number of grid points in x and θ directions respectively, which can be obtained by Chebyshev polynomials as follows (Ghorbanpour Arani *et al.* 2013, 2015c)

$$x_i = \frac{L}{2} \left[1 - \cos\left(\frac{i-1}{N_x - 1} \right) \pi \right], \quad i = 1, ..., N_x \quad (70)$$

$$\theta_i = \frac{2\pi}{2} \left[1 - \cos\left(\frac{i-1}{N_\theta - 1} \right) \pi \right]. \quad i = 1, ..., N_\theta \quad (71)$$

However, applying DQM to motion equations yields the following coupled matrix equations

$$[M] \begin{bmatrix} \ddot{Y}_b \\ \ddot{Y}_d \end{bmatrix} + \left(\underbrace{[C_L + C_{NL}]}_{[C]} \right) \begin{bmatrix} \dot{Y}_b \\ \dot{Y}_d \end{bmatrix} + \left(\underbrace{[K_L + K_{NL}]}_{[K]} \right) \begin{bmatrix} Y_b \\ Y_d \end{bmatrix} = \begin{bmatrix} 0 \\ 0 \end{bmatrix}, \quad (72)$$

where $[K]$ and $[K_{NL}]$ are the linear and nonlinear stiffness matrixes, respectively; $[C_L]$ and $[C_{NL}]$ are the linear and nonlinear damp matrixes, respectively; $[C]^f$ and $[K]^f$ are the respectively, damping and stiffness matrixes related to pulsating fluid; $[M]$ is the mass matrix; $\{Y\}$ is the displacement vector (i.e., $\{Y\} = \{u, v, w_b, w_s, \psi_x, \psi_\theta, \phi, \Phi\}$; subscript b and d represent boundary and domain points.

For solving the Eq. (72) and reducing it to the standard form of eigenvalue problem, it is convenient to rewrite Eq.

(72) as the following first order variable as

$$\{\dot{Z}\} = [A]\{Z\}, \tag{73}$$

in which the state vector Z and state matrix $[A]$ are defined as

$$Z = \begin{Bmatrix} d_d \\ \dot{d}_d \end{Bmatrix} \quad \text{and}$$

$$[A] = \begin{bmatrix} [0] & [I] \\ -[M^{-1}(K_L + K_{NL})] & -[M^{-1}(C_L + C_{NL})] \end{bmatrix} \tag{74}$$

where $[0]$ is the zero matrix; $[I]$ is the unitary matrix. Noted that the eigenvaluses obtained from Eq. (73) are complex which the imaginary and real parts are related to frequency and damping of structure, respectively.

6. Numerical result

A separator made from PVDF is considered with the mechanical and electrical properties listed in Table 1 (Ghorbanpour Arani *et al.* 2015b). The geometrical parameters of separator are considered as length to thickness ratio of $a/h = 20$ and thickness to radius ration of $h/R = 0.03$. In all of the figures, the dimensionless frequency

Table 1 Mechanical and electrical properties of PVDF

PVDF	SWCNT
$C_{11} = 238.24$ (GPa)	$E = 1$ (TPa)
$C_{22} = 23.6$ (GPa)	$\upsilon = 0.34$
$C_{12} = 3.98$ (GPa)	$\rho = 2300 \text{ kg/m}^3$
$C_{66} = 6.43$ (GPa)	
$e_{11} = -0.135$ (C/m^2)	
$e_{12} = -0.145$ (C/m^2)	
$\in = 1.1068 \times 10^{-8}$ (F/m)	
$\rho = 1780 \text{ kg/m}^3$	

$(\Omega = \omega h \sqrt{\rho/C_{11}})$ and dimensionless angular fluid velocity $(\Omega_f = \omega_f h \sqrt{\rho/C_{11}})$ are used. The key issue for successful application of the rule of mixture is to determine the SWCNT efficiency parameter η_j ($j = 1, 2, 3$). For short fibers, η_1 is usually taken to be 0.2 (Lei *et al.* 2014). However, there are no experiments conducted to determine the value of η_j for the PVDF matrix reinforced with SWCNTs. However, for parametric study, we chose from the reported values of Lei *et al.* (2014).
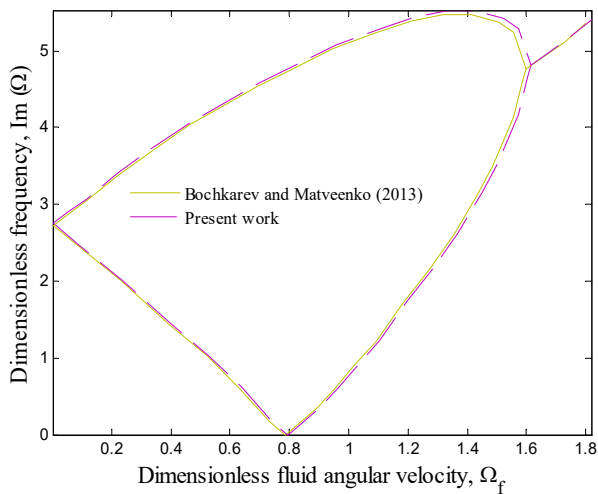
6.1 Validation

In this section, neglecting the piezoelectric properties, volume percent of SWCNT, structural damping and viscoelastic medium, the results are validated with the Bochkarev and Matveenko (2013a) for vibration and stability of cylindrical shell containing rotating fluid. The comparison results are shown in Figs. 2(a) and (b) for imaginary and real parts of eigenvalue. It can be seen that the present results are close to the results of Bochkarev and Matveenko (2013a), indication validation of present work. Noted that the little difference between this work and Bochkarev and Matveenko (2013a) is due to the different solution method (i.e., DQM in this work and finite element method in Bochkarev and Matveenko (2013a)).
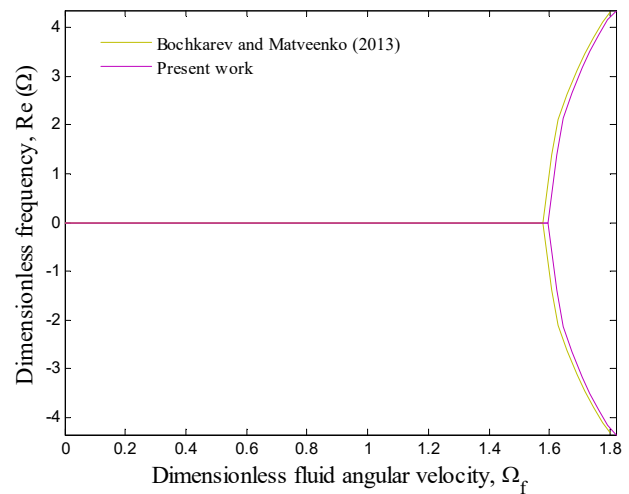
6.2 DQM Convergence

The convergence and accuracy of the DQM in evaluating the imaginary and real parts of eigenvalue are shown in Figs. 3(a) and (b) for CST, 3(c) and (d) for FSDT, 3(e) and (f) for SSDT for different grid point numbers. Fast rate of convergence of the methods are quite evident and it can be found that 15 and 17 grid points can yield accurate results in CST and FSDT-SSDT, respectively.

6.3 The effect of different parameters

In all of the figures, the imaginary and real parts of dimensionless eigenvalue are shown for different theories versus dimensionless fluid angular velocity for the

(a)

(b)

Fig. 2 Validation of present work with the result of Bochkarev and Matveenko (2013a)
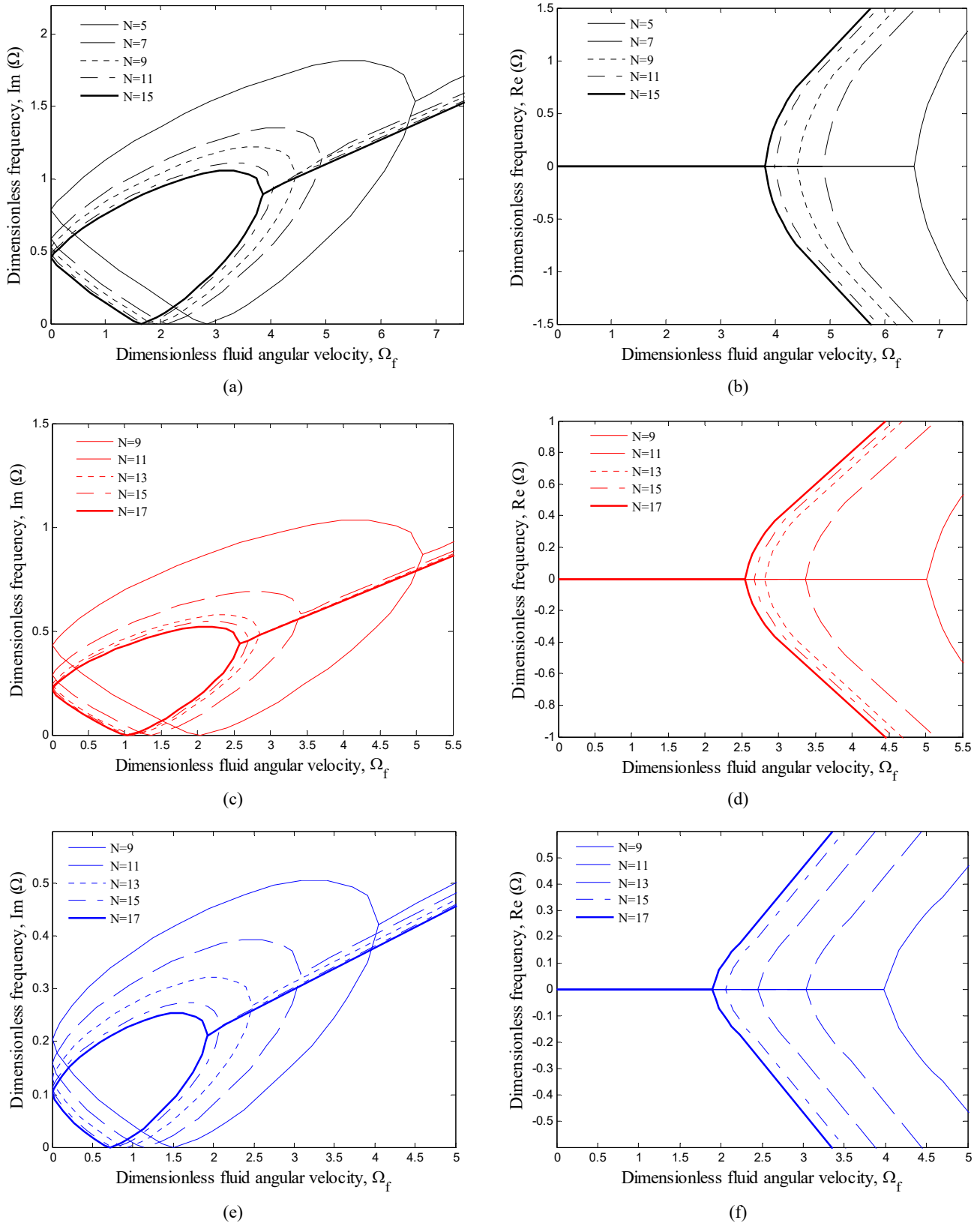
Fig. 3 Convergence and accuracy of DQM

SWCNTs volume percent of $\rho = V_{CNT} = 0.01$. Figs. 4-9(a)-(b), (c)-(d) and (e)-(f) are related to CST, FSDT and SSDT, respectively. Noted that the imaginary and real parts of eigenvalue are corresponded to frequency and damping of structure, respectively. Generally, the dimensionless frequency is divided to two parts of forward (the increasing part) and backward (the decreasing part) propagating waves. As can be seen at a special value of the dimension-
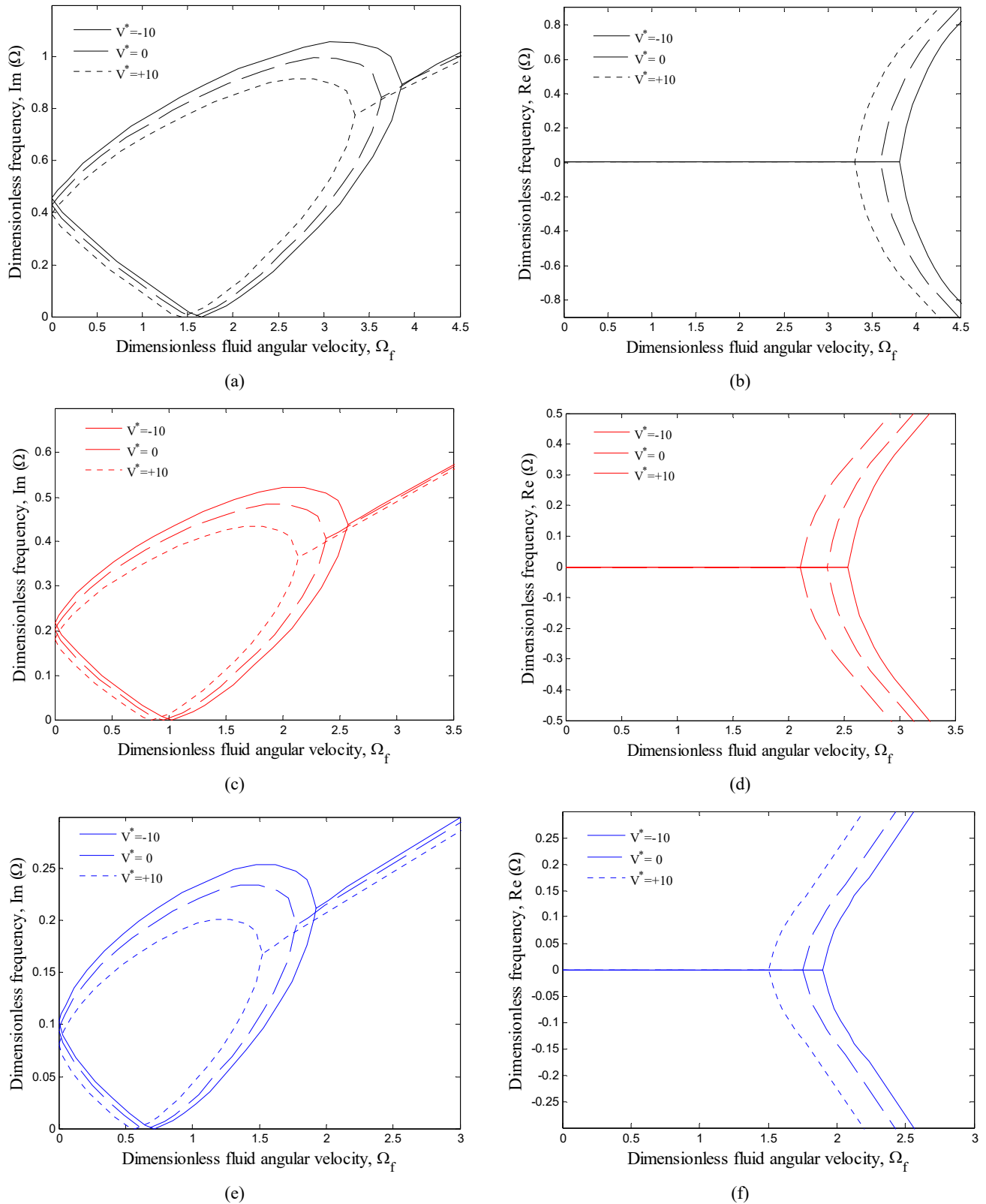
(a)

(b)

(c)

(d)

(e)

(f)

Fig. 4 The effects of external electric voltage on the imaginary and real parts of frequency
(a), (b): CST-(c), (d): FSDT-(e), (f): SSDT

less fluid angular velocity, the backward frequency reaches to zero and then grows until the forward and backward frequencies reach to each others at a certain dimensionless fluid angular velocity. In this state, the real part of the eigenvalue becomes positive and consequently, the flutter instability has been occurred.

Figs. 4(a) and (b), 4(c) and (d), 4(e) and (f) show the dimensionless eigenvalue, respectively corresponding to
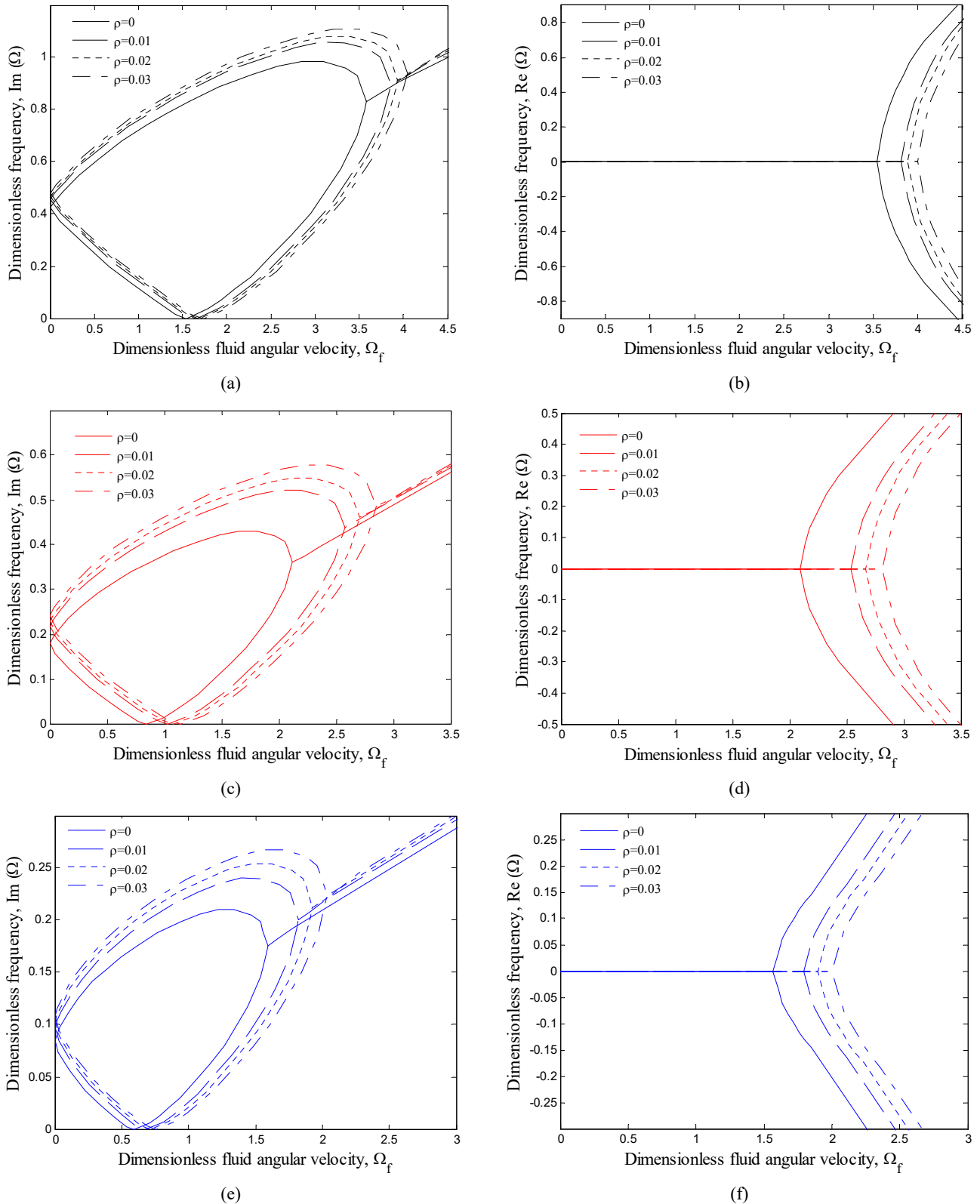
Fig. 5 The effects of SWCNT as reinforcer on the on the imaginary and real parts of frequency
(a), (b): CST-(c), (d): FSDT -(e), (f): SSDT

CST, FSDT and SSDT, for different dimensionless applied voltage ($V^* = V_0 / h / \sqrt{C_{11} / \in_{11}}$). It can be found that applying negative and positive voltages to separator, respectively increases and decreases dimensionless

frequency and critical angular fluid velocity. It is because applying negative voltage induces tensile force in structure while the positive one leads to a compressive force in separator. However, it can be concluded that the applied
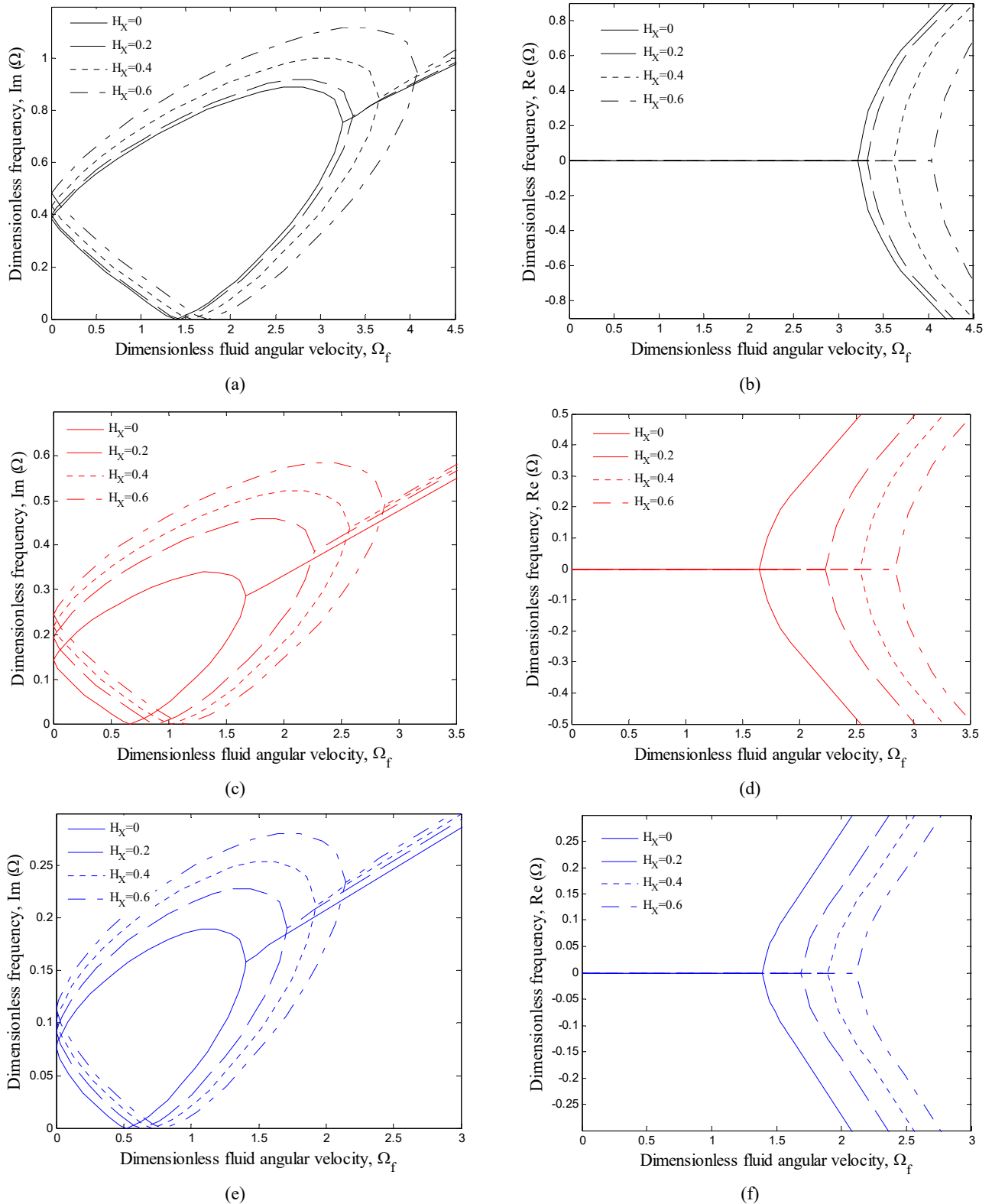
(a)

(b)

(c)

(d)

(e)

(f)

Fig. 6 The effects of magnetic field on the imaginary and real parts of frequency
(a), (b): CST-(c), (d): FSDT -(e), (f): SSDT

external voltage is an effective controlling parameter for vibration and stability smart control of separators conveying rotating fluid flow.

The SWCNT volume fraction effects (ρ) on the dimensionless imaginary and real parts of eigenvalue are

illustrated in Figs. 5(a) and (b) corresponding to CST, 5(c) and (d) corresponding FSDT, 5(e) and (f) corresponding to SSDT. As can be seen, the dimensionless frequency and critical angular fluid velocity of the separator are increased with reinforcing the structure with SWCNTs. In the other
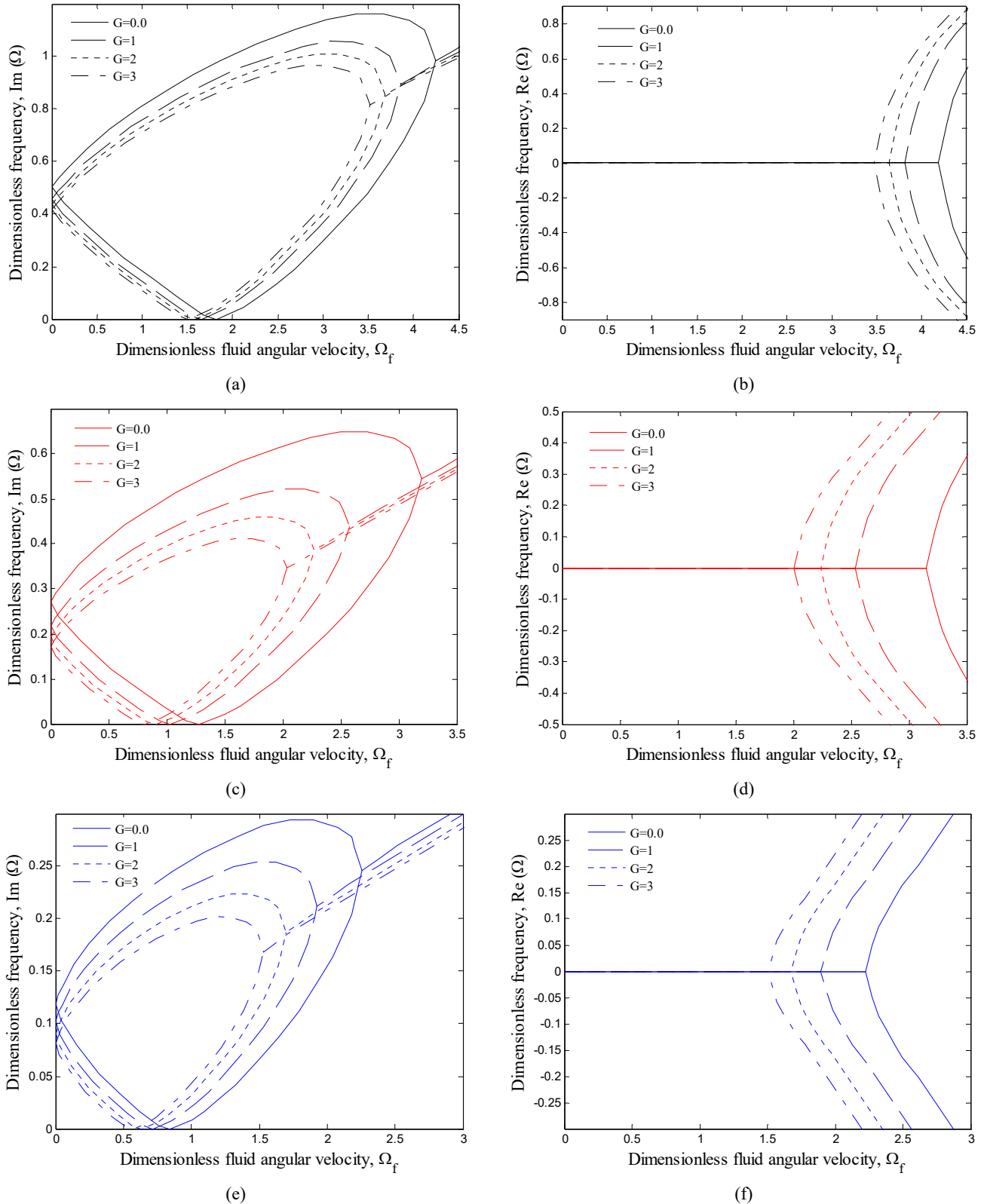
Fig. 7 The effects of structural damping on the imaginary and real parts of frequency
(a), (b): CST-(c), (d): FSDT -(e), (f): SSDT

words, increasing volume fraction of SWCNTs leads to higher dimensionless frequency and critical angular fluid velocity. Physically it means that with reinforcing the separator with SWCNT, the stiffness of structure increases.

In results, reinforcing the structure with SWCVT causes to delay in the flutter instability of structure.

Figs. 6(a) and (b), 6(c) and (d), 6(e) and (f) for CST, FSDT and SSDT, respectively are plotted for showing the
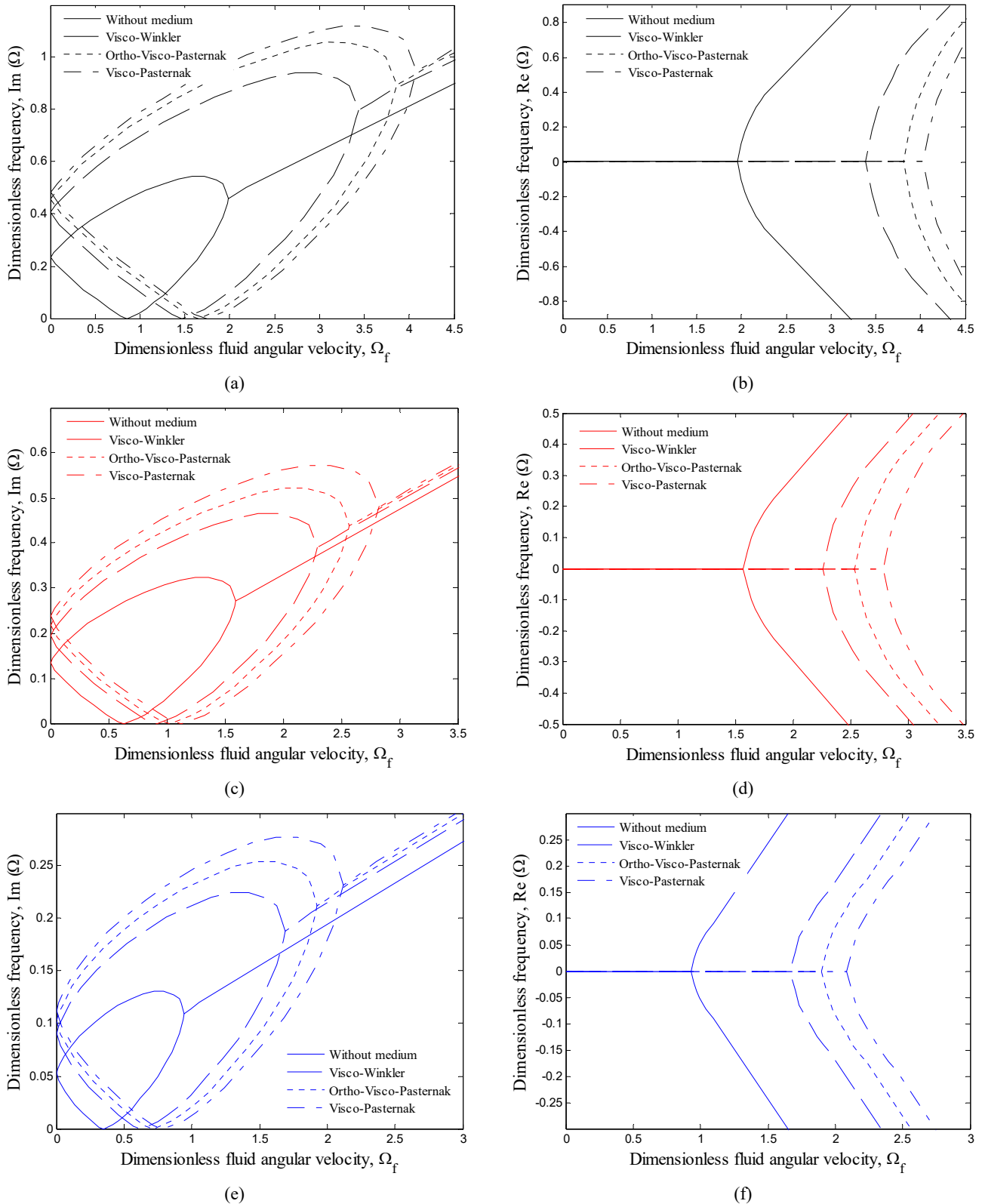
Fig. 8 The effects of viscoelastic medium type on the imaginary and real parts of frequency
(a), (b): CST-(c), (d): FSDT -(e), (f): SSDT

effect of dimensionless axial magnetic field ($H_X = H_x/C_{11}$) on the dimensionless frequency and critical angular fluid velocity of structure. Here, fourvalues of 0, 0.2, 0.4 and 0.6 are considered. It can be observed that with increasing the

dimensionless axial magnetic field, dimensionless critical angular fluid velocity and frequency will be increased. It is physically due to the fact that with increasing the dimensionless axial magnetic field, the stiffness of structure
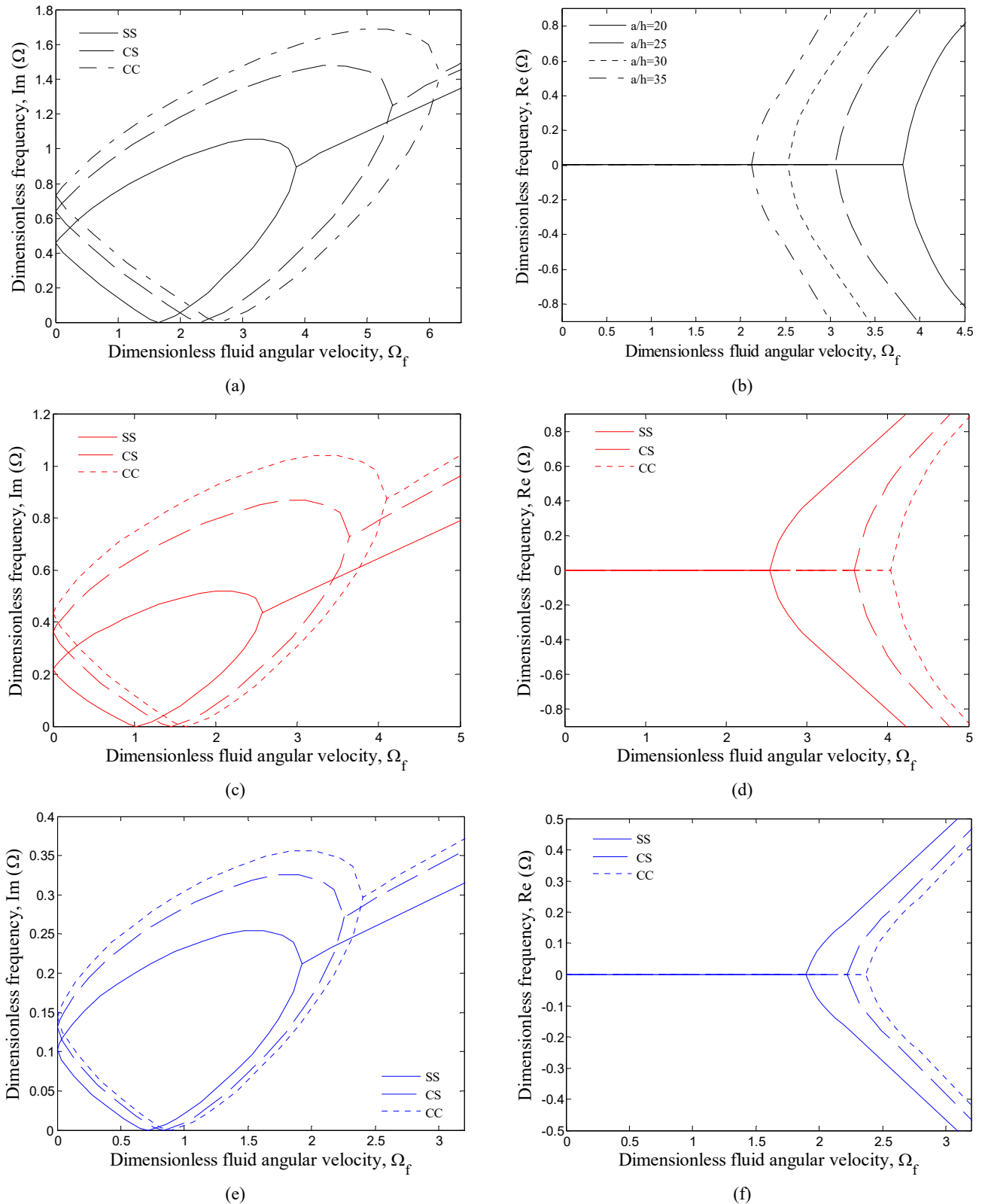
Fig. 9 The effects of boundary conditions on the imaginary and real parts of frequency
(a), (b): CST-(c), (d): FSDT -(e), (f): SSDT

increases.

For presenting the effect of dimensionless structural damping parameter ($G = g / h / C_{11} / \rho$), Figs. 7(a) and (b), 7(c) and (d), 7(e) and (f) for CST, FSDT and SSDT, respectively are plotted. As can be seen, with increasing dimensionless structural damping parameter, the dimensionless frequency and critical angular fluid velocity of system are decreased. It is due to the fact that with increasing
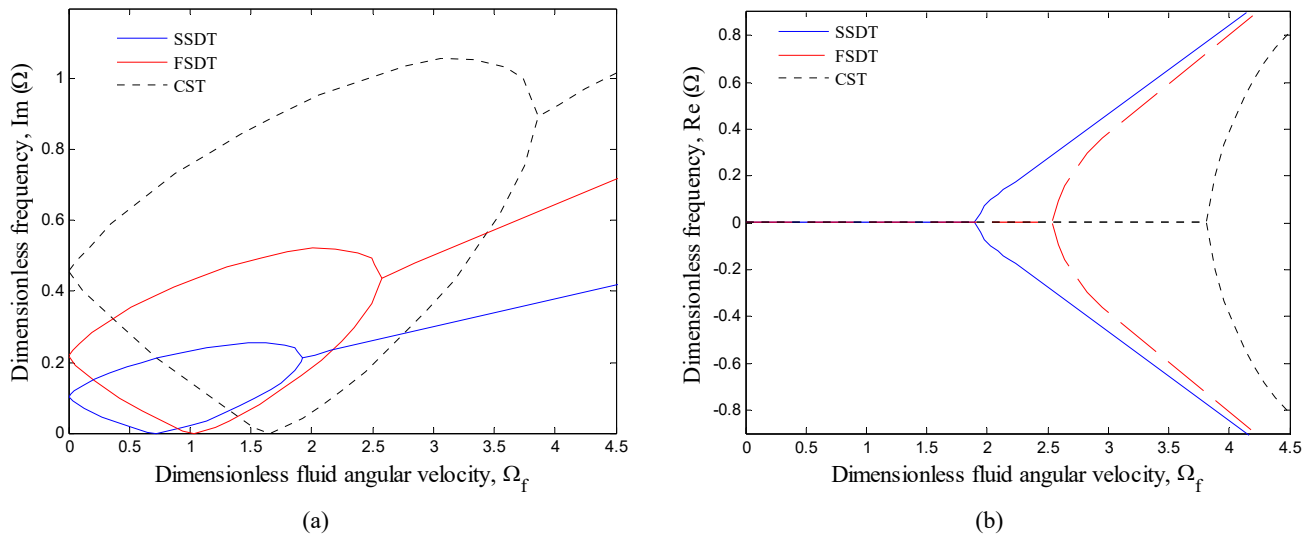
Fig. 10 Comparison of imaginary and real parts of frequency (a), (b): CST-(c), (d): FSDT -(e), (f): SSDT

dimensionless structural damping parameter, the damping force which results in more absorption of energy by the system will be induced.

In order to show the effects of surrounding viscoelastic foundation, Figs. 8(a) and (b) for CST, 8(c) and (d) for FSDT, 8(e) and (f) for SSDT are shown. Four different viscoelastic medium are considered namely as without medium, Visco-Winkler, orthotropic visco-Pasternak and orthotropic Pasternak. As can be seen considering elastic foundation increases the dimensionless frequency and critical angular fluid velocity of separators. Physically it means that putting the separatorin a viscoelastic medium makes it more stable and stiffer. It is also observed that the dimensionless frequency and critical angular fluid velocity of orthotropic visco-Pasternak or visco-Pasternak model is higher than Visco-Winkler one. It is due to the fact that Pasternak model considers not only the normal stresses but also the transverse shear deformation and continuity among the spring elements. In addition, the frequency and critical angular fluid velocity predicted by orthotropic visco-Pasternak medium is lower than visco-Pasternak one. It is because in orthotropic visco-Pasternak medium, the shear layer is considered with the angle of 45 degree.

Figs. 9(a) and (b), 6(c) and (d), 6(e) and (f) for CST, FSDT and SSDT, respectively are plotted for presenting the effect of different boundary conditions on the dimensionless frequency and critical angular fluid velocity of structure. Here, three boundary conditions of SS, CS and CC are considered. It can be observed that for the CC separator, the dimensionless critical angular fluid velocity and frequency are higher than CS and SS separators. It is physically due to the fact that for the CC boundary conditions, the stiffness of structure increases.

A comparison of three different theories in predicting the dimensionless frequency and critical angular fluid velocity is presented in Figs. 10(a) and (b) corresponding to CST, 10(c) and (d) corresponding FSDT, 10(e) and (f) corresponding to SSDT. It can be found that the dimensionless frequency and critical angular fluid velocity predicted by SSDT are lower than FSDT and CST. It is perhaps due to

the fact that the flexibility of structure modeled by SSDT is lower that other theories. Furthermore, the displacement field in SSDT is close to the deflection of structure and it can be another reason for more accuracy of this theory. It can be also found that the results calculated by CST are much overestimated with respect to FSDT and SSDT.

7. Conclusions

Assessment of CST, FSDT and SSDT for nonlinear vibration and stability analysis of piezoelectric nano-composite separators containing rotating fluid was achieved in the present work. To consider the structural damping effects in the structure, Kelvin–Voigt theory was incorporated. The behavior of the rotating fluid was described in the framework of the potential theory and linearized Bernoulli formula. The separator was subjected to 3D electric and 2D magnetic fields and was surrounded by nonlinear orthotropic visco Pasternak foundation. Numerical simulation is done using a DQM for calculating the dimensionless frequency and critical angular fluid velocity. The effects of different parameters such as external voltage, magnetic field, visco-Pasternak foundation, structural damping and volume percent of SWCNTs were shown on the vibration and stability of structure. Numerical results shown that at a special value of the dimensionless fluid angular velocity, the forward and backward frequencies reach to each other's which the flutter instability was occurred. It can be found that applying negative and positive voltages to separator, respectively increases and decreases dimensionless frequency and critical angular fluid velocity. The dimensionless frequency and critical angular fluid velocity of the separator were increased with reinforcing the structure with SWCNTs. It can be observed that with increasing the dimensionless axial magnetic field, dimensionless critical angular fluid velocity and frequency will be increased. In addition, with increasing dimensionless structural damping parameter, the dimensionless frequency and critical angular fluid velocity

of system were decreased. It can be also found that the dimensionless frequency and critical angular fluid velocity predicted by SSDT were lower than FSDT and CST. The results of this study were validated by Bochkarev and Matveenko (2013a). Finally, it was hoped that the results of this paper would be beneficial for the design of separators used in oil and gas industries.

Acknowledgement

References

Amabili, M. (2008), *Nonlinear Vibrations and Stability of Shells and Plates*, Cambridge University Press, New York, NY, USA.

Amabili, M. (2011), "Nonlinear vibrations of laminated circular cylindrical shells, Comparison of different shell theories", *Compos. Struct.*, **94**, 207-220.

Amabili, M., Pellicano, F. and Païdoussis, M.P. (2001), "Nonlinear stability of circular cylindrical shells in annular and unbounded axial flow", *J. Appl. Mech.*, **68**, 827-834.

Bahadori, R. and Najafizadeh, M.M. (2015), "Free vibration analysis of two-dimensional functionally graded axisymmetric cylindrical shell on Winkler–Pasternak elastic foundation by First-order Shear Deformation Theory and using Navier-differential quadrature solution methods", *Appl. Math. Model.*, **39**(16), 4877-4894.

Bert, C.W. and Malik, M. (1996), "Differential quadrature method in computational mechanics: A review", *Appl. Mech. Rev.*, **49**, 1-27.

Bochkarev, S.A. and Matveenko, V.P. (2012a), "Stability analysis of stationary and rotating circular cylindrical shells conveying flowing and rotating fluid", *Mech. Solids*, **47**(5), 560-565.

Bochkarev, S.A. and Matveenko, V.P. (2012b), "Stability analysis of cylindrical shells containing a fluidwith axial and circumferential velocity components", *J. Appl. Mech. Tech. Phys.*, **53**(5), 768-776.

Bochkarev, S.A. and Matveenko, V.P. (2013a), "Numerical analysis of stability of a stationary or rotating circular cylindrical shell containing axially flowing and rotating fluid International", *J. Mech. Sci. Thech.*, **68**, 258-269.

Bochkarev, S.A. and Matveenko, V.P. (2013b), "Stability of a cylindrical shell subject to an annular flowof rotating fluid", *J. Sound Vib.*, **332**(18), 4210-4222.

Chen, T.L.C. and Bert, C.W. (2010), "Dynamic stability of isotropic or composite-material cylindrical shells containing swirling fluid flow", *J. Appl. Mech.*, **44**, 112-116.

Cortelezzi, L., Pong, A. and Paıdoussis, M.P. (2004), "Flutter of rotating shells with aco-rotating axial flow", *J. Appl. Mech.*, **71**(1), 143-145.

Dong, K. and Wang, X. (2006), "Wave propagation in laminated piezoelectric cylindrical shells in hydrothermal environment", *Struct. Eng. Mech., Int. J.*, **24**(4), 395-410.

Dowell, E.H., Srinivasan, A.V., McLean, J.D. and Ambrose, J. (1974), "Aeroelastic stability ofcylindrical shells subjected to a rotating flow", *AIAA J.*, **12**(12), 1644-1651.

Fantuzzi, N., Bacciocchi, M., Tornabene, F., Viola, E. and Ferreira, A.J.M. (2015), "Radial basis functions based on differential quadrature method for the free vibration analysis of laminated composite arbitrarily shaped plates", *Compos. Part B*: *Eng.*, **78**, 65-78.

Formica, G., Lacarbonara, W. and Alessi, R. (2010), "Vibrations of carbon nanotube reinforced composites", *J. Sound Vib.*, **329**(10), 1875-1889.

Fukuda, H. and Kawata, K. (1974), "On Young's modulus of short fibre composites", *Fibre Sci. Technol.*, **7**(3), 207-222.

Ganesan, R. and Ramu, S.A. (1995), "Vibration and stability of fluid conveying pipes with stochastic parameters", *Struct. Eng. Mech., Int. J.*, **3**(4), 313-324.

Ghorbanpour Arani, A., Haghshenas, E., Amir, S., Mozdianfard, M.R. and Latifi, M. (2013a), "Electro-thermo-mechanical response of thick-walled piezoelectric cylinder reinforced by boron-nitride nanotubes", *Streng. Mat.*, **45**(1), 102-115.

Ghorbanpour Arani, A., Kolahchi, R. and Khoddami Maraghi, Z. (2013b), "Nonlinear vibration and instability of embedded double-walled boron nitride nanotubes based on nonlocal cylindrical shell theory", *Appl. Math. Model.*, **37**(14), 7685-7707.

Ghorbanpour Arani, A., Haghparast, E., Khoddami Maraghi, Z. and Amir, S. (2015a), "Static stress analysis of carbon nano-tube reinforced composite CNTRC cylinder under non-axisymmetric thermo-mechanical loads and uniform electro-magnetic fields", *Compos. Part B*, **68**, 136-145.

Ghorbanpour Arani, A., Abdollahian, M. and Kolahchi, R. (2015b), "Nonlinear vibration of embedded smart composite microtube conveying fluid based on modified couple stress theory", *Polym. Compos.*, **36**(7), 1314-1324.

Ghorbanpour Arani, A., Kolahchi, R. and Zarei, M.Sh. (2015c), "Visco-surface-nonlocal piezoelasticity effects on nonlinear dynamic stability of graphene sheets integrated with ZnO sensors and actuators using refined zigzag theory", *Compos. Struct.*, **132**, 506-526.

Ghorbanpour Arani, A., Karimi, M.S. and Rabani Bidgoli, M. (2016), "Nonlinear vibration and instability of rotating piezoelectric nano-composite sandwich cylindrical shells containing axially flowing and rotating fluid-particle mixture", *Polym. Compos.*

Gosselin, F. and Païdoussis, M.P. (2009), "Blocking in the rotating axial flow in a co-rotatingflexible shell", *J. Appl. Mech.*, **76**(1), 011001.

Gupta, U.S., Lal, R. and Sharma, S. (2006), "Vibration analysis of non-homogeneous circular plate of nonlinear thickness variation by differential quadrature method", *J. Sound Vib.*, **298**(4), 892-906.

Jalili, N. (2010), *Piezoelectric-Based Vibration Control from Macro to Micro/Nano Scale Systems Springer Science*, New York.

Kumar, D. and Srivastava, A. (2016), "Elastic properties of CNT- and graphene-reinforced nanocomposites using RVE ", *Steel Compos. Struct., Int. J.*, **21**(5), 1085-1103.

Lei, Z.X., Zhang, L.W., Liew, K.M. and Yu, J.L. (2014), "Dynamic stability analysis of carbon nanotube-reinforced functionally graded cylindrical panels using the element-free kp-Ritz method", *Compos. Struct.*, **113**, 328-338.

Liew, K.M. and Liu, F.L. (2000), "Differential quadrature method for vibration analysis of shear deformable annular sector plates", *J. Sound Vib.*, **230**(2), 335-356.

Mantari, J.L. and Guedes Soares, C. (2014), "Optimized sinusoidal higher order shear deformation theory for the analysis of functionally graded plates and shells", *Compos. Part B*, **56**, 126-136.

Nie, G. and Zhong, Z. (2007), "Semi-analytical solution for three-dimensional vibration of functionally graded circular plates", *Comput. Methods Appl. Mech. Eng.*, **196**(49), 4901-4910.

Nie, G. and Zhong, Z. (2010), "Dynamic analysis of multi-directional functionally graded annular plate", *Appl. Math. Model.*, **34**(3), 608-616.

Païdoussis, M.P., Misra, A.K. and Nguyen, V.B. (1992), "Internal-

and annular-flow-induced instabilities of a clamped–clamped or cantilevered cylindrical shell in acoaxial conduit, the effects of system parameters", *J. Sound Vib.*, **159**(2), 193-205.

Rabani Bidgoli, M., Karimi, M.S. and Ghorbanpour Arani, A. (2016), "Viscous fluid induced vibration and instability of FG-CNT-reinforced cylindrical shells integrated with piezoelectric layers", *Steel Compos. Struct., Int. J.*, **19**(3), 713-733.

Sofiyev, A.H. (2011), "Thermal buckling of FGM shells resting on a two-parameter elastic foundation", *Thin-Wall. Struct.*, **49**(10), 1304-1311.

Sofiyev, A.H. (2016), "Nonlinear free vibration of shear deformable orthotropic functionally graded cylindrical shells", *Compos. Struct.*, **14**2, 35-44.

Sun, A., Xu, X., Lim, C.W., Zhou, Zh. and Xiao, Sh. (2016), "Accurate thermo-electro-mechanical buckling of shear deformable piezoelectric fiber-reinforced composite cylindrical shells", *Compos. Struct.*, **141**, 221-231.

Tahouneh, V. (2016), "Using an equivalent continuum model for 3D dynamic analysis of nanocomposite plates", *Steel Compos. Struct., Int. J.*, **20**(3), 623-649.

Tahouneh, V. and Yas, M.H. (2014), "Influence of equivalent continuum model based on the Eshelby-Mori-Tanaka scheme on the vibrational response of elastically supported thick continuously graded carbon nanotube-reinforced annular plates", *Polym. Compos.*, **35**(8), 1644-1661.

Tahouneh, V., Yas, M.H., Tourang, H. and Kabirian, M. (2013), "Semi-analytical solution for three-dimensional vibration of thick continuous grading fiber reinforced (CGFR) annular plates on Pasternak elastic foundations with arbitrary boundary conditions on their circular edges", *Meccanica*, **48**(6), 1313-1336.

Thai, H.T. and Vo, T.P. (2013), "A new sinusoidal shear deformation theory for bending, buckling, and vibration of functionally graded plates", *Appl. Math. Model.*, **37**(5), 3269-3281.

Tornabene, F. and Ceruti, A. (2013), "Mixed static and dynamic optimization of four-parameter functionally graded completely doubly curved and degenerate shells and panels using GDQ method", *Math. Prob. Eng.*, **2013**, 1-33.

Yang, H., Jin, G., Liu, Zh., Wang, X. and Miao, X. (2015), "Vibration and damping analysis of thick sandwich cylindrical shells with a viscoelastic core under arbitrary boundary conditions", *Int. J. Mech. Sci.*, **92**, 162-177.

CC

Appendix A

The Lorentz force due to a steady magnetic field, H_0 can be obtained as follows (GhorbanpourArani *et al.* 2015c)

$$f_m = \eta \left(\nabla \times \underbrace{\left(\nabla \times \underbrace{(u \times H_0)}_{h} \right)}_{J} \right) \times H_0, \tag{A1}$$

where η, ∇, u, h and J are the magnetic permeability of the SWCNTs, gradient operator, displacement field vector, disturbing vectors of magnetic field and current density, respectively. Noted that in this paperthe magnetic field isassumed as $H_0 = H_x \delta_{x\vartheta} \hat{e}_x + H_\theta \delta_{\theta\vartheta} \hat{e}_\theta$ where δ is the Kronecker delta tensor. The generated forces and the bending moment caused by Lorentz force may be calculated by

$$\left(R_x^m, R_\theta^m, R_z^m \right) = \int_{-h/2}^{h/2} (f_x, f_\theta, f_z) dz, \tag{A2}$$

$$\left(M_x^m, M_\theta^m, M_z^m \right) = \int_{-h/2}^{h/2} (f_x, f_\theta, f_z) z dz, \tag{A3}$$

Using Eqs. (14a)-(14c), the Lorentz force per unit volume for CST can be calculated as

$$f_x = \eta H_\theta^2 \delta_{\theta\vartheta} \left[\left(\frac{\partial^2 u}{\partial x^2} + \frac{\partial^2 u}{R^2 \partial \theta^2} \right) - z \left(\frac{\partial^3 w}{\partial x^3} + \frac{\partial^3 w}{R^2 \partial x \partial \theta^2} \right) \right], \tag{A4}$$

$$f_\theta = \eta H_x^2 \delta_{x\vartheta} \left[\left(\frac{\partial^2 v}{\partial x^2} + \frac{\partial^2 v}{R^2 \partial \theta^2} \right) - z \left(\frac{\partial^3 w}{R^3 \partial \theta^3} + \frac{\partial^3 w}{R \partial \theta \partial x^2} \right) \right], \tag{A5}$$

$$f_z = \eta \left[H_\theta^2 \delta_{\theta\vartheta} \left(\frac{\partial^2 w}{R^2 \partial \theta^2} - \frac{\partial^2 w}{\partial x^2} \right) + H_x^2 \delta_{x\vartheta} \left(\frac{\partial^2 w}{\partial x^2} - \frac{\partial^2 w}{R^2 \partial \theta^2} \right) \right]. \tag{A6}$$

Using Eqs. (31a)-(31c), the Lorentz force per unit volume for FSDT can be expressed as

$$f_x = \eta H_\theta^2 \delta_{\theta\vartheta} \left[\left(\frac{\partial^2 u}{\partial x^2} + \frac{\partial^2 u}{R^2 \partial \theta^2} \right) + z \left(\frac{\partial^2 \psi_x}{\partial x^2} + \frac{\partial^2 \psi_x}{R^2 \partial \theta^2} \right) \right], \tag{A7}$$

$$f_\theta = \eta H_x^2 \delta_{x\vartheta} \left[\left(\frac{\partial^2 v}{\partial x^2} + \frac{\partial^2 v}{R^2 \partial \theta^2} \right) + z \left(\frac{\partial^2 \psi_\theta}{R^2 \partial \theta^2} + \frac{\partial^2 \psi_\theta}{\partial x^2} \right) \right], \tag{A8}$$

$$f_z = \eta \left[H_\theta^2 \delta_{\theta\vartheta} \left(\frac{\partial^2 w}{\partial x^2} + \frac{\partial \psi_\theta}{R \partial \theta} \right) + H_x^2 \delta_{x\vartheta} \left(\frac{\partial^2 w}{\partial x^2} + \frac{\partial \psi_\theta}{R \partial \theta} \right) \right]. \tag{A9}$$

Using Eqs. (46a)-(46c), the Lorentz force per unit volume for SSDTcan be expressed as

$$\begin{aligned} f_x = \eta H_\theta^2 \delta_{\theta\vartheta} &\left[\left(\frac{\partial^2 u}{\partial x^2} + \frac{\partial^2 u}{R^2 \partial \theta^2} \right) \right. \\ &\left. - z \left(\frac{\partial^3 w_b}{\partial x^3} + \frac{\partial^3 w}{R^2 \partial x \partial \theta^2} \right) - f \left(\frac{\partial^3 w_s}{\partial x^3} + \frac{\partial^3 w_s}{R^2 \partial x \partial \theta^2} \right) \right], \end{aligned} \tag{A10}$$

$$\begin{aligned} f_\theta = \eta H_x^2 \delta_{x\vartheta} &\left[\left(\frac{\partial^2 v}{\partial x^2} + \frac{\partial^2 v}{R^2 \partial \theta^2} \right) \right. \\ &\left. - z \left(\frac{\partial^3 w_b}{R^3 \partial \theta^3} + \frac{\partial^3 w_b}{R \partial \theta \partial x^2} \right) - f \left(\frac{\partial^3 w_s}{R^3 \partial \theta^3} + \frac{\partial^3 w_s}{R \partial \theta \partial x^2} \right) \right], \end{aligned} \tag{A11}$$

$$\begin{aligned} f_z = \eta &\left[H_\theta^2 \delta_{\theta\vartheta} \left(\frac{\partial^2 w_b}{R^2 \partial \theta^2} + \frac{\partial^2 w_s}{R^2 \partial \theta^2} - \frac{\partial^2 w_b}{\partial x^2} - (1-p) \frac{\partial^2 w_s}{\partial x^2} \right) \right. \\ &\left. + H_x^2 \delta_{x\vartheta} \left(\frac{\partial^2 w_b}{\partial x^2} + \frac{\partial^2 w_s}{\partial x^2} - \frac{\partial^2 w_b}{R^2 \partial \theta^2} - (1-p) \frac{\partial^2 w_s}{R^2 \partial \theta^2} \right) \right]. \end{aligned} \tag{A12}$$

Appendix B

The resultant force and moments may be calculated as

$$
\begin{bmatrix} N_{xx} \\ N_{\theta\theta} \\ N_{x\theta} \\ Q_x \\ Q_\theta \end{bmatrix} = \int_{-h/2}^{h/2} \begin{bmatrix} \sigma_{xx} \\ \sigma_{\theta\theta} \\ \sigma_{x\theta} \\ k'\sigma_{xz} \\ k'\sigma_{z\theta} \end{bmatrix} dz,
\tag{B1}
$$

$$
\begin{bmatrix} M_{xx} \\ M_{\theta\theta} \\ M_{x\theta} \end{bmatrix} = \int_{-h/2}^{h/2} \begin{bmatrix} \sigma_{xx} \\ \sigma_{\theta\theta} \\ \sigma_{x\theta} \end{bmatrix} z\,dz,
\tag{B2}
$$

$$
\begin{bmatrix} S_{xx} \\ S_{\theta\theta} \\ S_{x\theta} \end{bmatrix} = \int_{-h/2}^{h/2} \begin{bmatrix} \sigma_{xx} \\ \sigma_{\theta\theta} \\ \sigma_{x\theta} \end{bmatrix} f\,dz,
\tag{B3}
$$

$$
\begin{bmatrix} F_{xx} \\ F_{\theta\theta} \end{bmatrix} = \int_{-h/2}^{h/2} \begin{bmatrix} \sigma_{xx} \\ \sigma_{\theta\theta} \end{bmatrix} p\,dz,
\tag{B4}
$$

where k' is shear correction factor which used in FSDT. Furthermore, the moment of inertia in kinetic energy of three theories can be defined as

$$
(I_0, I_1, I_2, I_3, I_4, I_5) = \int_{-h/2}^{h/2} \rho(1, z, z^2, f^2, zf, f)\,dz.
\tag{B5}
$$

Using Eqs. (16) and (17), the resultant force and moments for CST can be written as

$$
N_{xx} = A_{11}\left(\frac{\partial u}{\partial x} + \frac{1}{2}\left(\frac{\partial w}{\partial x}\right)^2\right) - B_{11}\left(\frac{\partial^2 w}{\partial x^2}\right)
$$
$$
+ A_{12}\left(\frac{\partial v}{R\partial\theta} + \frac{w}{R} + \frac{1}{2}\left(\frac{\partial w}{R\partial\theta}\right)^2\right) - B_{12}\left(\frac{\partial^2 w}{R^2\partial\theta^2}\right) + F_{310}\varphi,
\tag{B6}
$$

$$
N_{\theta\theta} = A_{12}\left(\frac{\partial u}{\partial x} + \frac{1}{2}\left(\frac{\partial w}{\partial x}\right)^2\right) - B_{12}\left(\frac{\partial^2 w}{\partial x^2}\right)
$$
$$
+ A_{22}\left(\frac{\partial v}{R\partial\theta} + \frac{w}{R} + \frac{1}{2}\left(\frac{\partial w}{R\partial\theta}\right)^2\right) - B_{22}\left(\frac{\partial^2 w}{R^2\partial\theta^2}\right) + F_{320}\varphi,
\tag{B7}
$$

$$
N_{x\theta} = A_{66}\left(\frac{\partial u}{R\partial\theta} + \frac{\partial v}{\partial x} + \frac{\partial w}{\partial x}\frac{\partial w}{R\partial\theta}\right) - B_{66}\left(2\frac{\partial^2 w}{R\partial x\partial\theta}\right),
\tag{B8}
$$

$$
M_{xx} = B_{11}\left(\frac{\partial u}{\partial x} + \frac{1}{2}\left(\frac{\partial w}{\partial x}\right)^2\right) - D_{11}\left(\frac{\partial^2 w}{\partial x^2}\right)
$$
$$
+ B_{12}\left(\frac{\partial v}{R\partial\theta} + \frac{w}{R} + \frac{1}{2}\left(\frac{\partial w}{R\partial\theta}\right)^2\right) - D_{12}\left(\frac{\partial^2 w}{R^2\partial\theta^2}\right) + F_{311}\varphi,
\tag{B9}
$$

$$
M_{\theta\theta} = B_{12}\left(\frac{\partial u}{\partial x} + \frac{1}{2}\left(\frac{\partial w}{\partial x}\right)^2\right) - D_{12}\left(\frac{\partial^2 w}{\partial x^2}\right)
$$
$$
+ B_{22}\left(\frac{\partial v}{R\partial\theta} + \frac{w}{R} + \frac{1}{2}\left(\frac{\partial w}{R\partial\theta}\right)^2\right) - D_{22}\left(\frac{\partial^2 w}{R^2\partial\theta^2}\right) + F_{321}\varphi,
\tag{B10}
$$

$$
M_{x\theta} = B_{66}\left(\frac{\partial u}{R\partial\theta} + \frac{\partial v}{\partial x} + \frac{\partial w}{\partial x}\frac{\partial w}{R\partial\theta}\right) - D_{66}\left(2\frac{\partial^2 w}{R\partial x\partial\theta}\right),
\tag{B11}
$$

$$
G_x = \frac{\in_{11}}{2}\frac{h}{\partial x}\frac{\partial\varphi}{\partial x},
\tag{B12}
$$

$$
G_\theta = \frac{\in_{22}}{2}\frac{h}{R\partial\theta}\frac{\partial\varphi}{R\partial\theta},
\tag{B13}
$$

$$
G_z = \frac{2h}{\pi}e_{32}\frac{\partial^2 w}{R^2\partial\theta^2} + \frac{2h}{\pi}e_{31}\frac{\partial^2 w}{\partial x^2} + \frac{\pi^2}{h}\varphi,
\tag{B14}
$$

Using Eqs. (33) and (34), the resultant force and moments for FSDT can be written as

$$
N_{xx} = A_{11}\left(\frac{\partial u}{\partial x} + \frac{1}{2}\left(\frac{\partial w}{\partial x}\right)^2\right) + B_{11}\left(\frac{\partial\psi_x}{\partial x}\right)
$$
$$
+ A_{12}\left(\frac{\partial v}{R\partial\theta} + \frac{w}{R} + \frac{1}{2}\left(\frac{\partial w}{R\partial\theta}\right)^2\right) + B_{12}\left(\frac{\partial\psi_\theta}{R\partial\theta}\right) + F_{310}\varphi,
\tag{B15}
$$

$$
N_{\theta\theta} = A_{12}\left(\frac{\partial u}{\partial x} + \frac{1}{2}\left(\frac{\partial w}{\partial x}\right)^2\right) + B_{12}\left(\frac{\partial\psi_x}{\partial x}\right)
$$
$$
+ A_{22}\left(\frac{\partial v}{R\partial\theta} + \frac{w}{R} + \frac{1}{2}\left(\frac{\partial w}{R\partial\theta}\right)^2\right) + B_{22}\left(\frac{\partial\psi_\theta}{R\partial\theta}\right) + F_{320}\varphi,
\tag{B16}
$$

$$
N_{x\theta} = A_{66}\left(\frac{\partial u}{R\partial\theta} + \frac{\partial v}{\partial x} + \frac{\partial w}{\partial x}\frac{\partial w}{R\partial\theta}\right)
$$
$$
+ B_{66}\left(\frac{\partial\psi_x}{R\partial\theta} + \frac{\partial\psi_\theta}{\partial x}\right),
\tag{B17}
$$

$$
Q_x = A_{55}\left(\frac{\partial w}{\partial x} + \psi_x\right) - G_{150}\frac{\partial\varphi}{\partial x},
\tag{B18}
$$

$$
Q_\theta = A_{44}\left(\frac{\partial w}{R\partial\theta} - \frac{v}{R} + \psi_\theta\right) - G_{240}\frac{\partial\varphi}{R\partial\theta},
\tag{B19}
$$

$$
M_{xx} = B_{11}\left(\frac{\partial u}{\partial x} + \frac{1}{2}\left(\frac{\partial w}{\partial x}\right)^2\right) + D_{11}\left(\frac{\partial\psi_x}{\partial x}\right)
$$
$$
+ B_{12}\left(\frac{\partial v}{R\partial\theta} + \frac{w}{R} + \frac{1}{2}\left(\frac{\partial w}{R\partial\theta}\right)^2\right) + D_{12}\left(\frac{\partial\psi_\theta}{R\partial\theta}\right) + F_{311}\varphi,
\tag{B20}
$$

$$M_{\theta\theta} = B_{12}\left(\frac{\partial u}{\partial x} + \frac{1}{2}\left(\frac{\partial w}{\partial x}\right)^2\right) + D_{12}\left(\frac{\partial \psi_x}{\partial x}\right)$$
$$+ B_{22}\left(\frac{\partial v}{R\partial\theta} + \frac{w}{R} + \frac{1}{2}\left(\frac{\partial w}{R\partial\theta}\right)^2\right) + D_{22}\left(\frac{\partial \psi_\theta}{R\partial\theta}\right) + F_{321}\varphi, \tag{B21}$$

$$M_{x\theta} = B_{66}\left(\frac{\partial u}{R\partial\theta} + \frac{\partial v}{\partial x} + \frac{\partial w}{\partial x}\frac{\partial w}{R\partial\theta}\right)$$
$$+ D_{66}\left(\frac{\partial \psi_x}{R\partial\theta} + \frac{\partial \psi_\theta}{\partial x}\right), \tag{B22}$$

$$G_x = \frac{2e_{15}h}{\pi}\frac{\partial w}{\partial x} + \frac{2e_{15}h}{\pi}\psi_x + \frac{\in_{11}}{2}\frac{h}{\partial x}\frac{\partial\varphi}{\partial x}, \tag{B23}$$

$$G_\theta = \frac{2e_{24}h}{\pi}\frac{\partial w}{R\partial\theta} - \frac{2e_{24}h}{\pi}\frac{v}{R} + \frac{2e_{24}h}{\pi}\psi_\theta$$
$$+ \frac{\in_{22}}{2}\frac{h}{R\partial\theta}\frac{\partial\varphi}{R\partial\theta}, \tag{B24}$$

$$G_z = \frac{2he_{32}}{\pi}\frac{\partial^2 w}{R^2\partial\theta^2} - \frac{2h}{\pi}e_{31}\frac{\partial\psi_x}{\partial x} + \frac{\pi^2}{2h}\in_{33}\varphi, \tag{B25}$$

Using Eqs. (48) and (49), the resultant force and moments for SSDT can be written as

$$N_{xx} = A_{11}\left(\frac{\partial u}{\partial x} + \frac{1}{2}\left(\frac{\partial w_b}{\partial x}\right)^2 + \frac{1}{2}\left(\frac{\partial w_s}{\partial x}\right)^2\right)$$
$$- B_{11}\left(\frac{\partial^2 w_b}{\partial x^2}\right) - E_{11}\left(\frac{\partial^2 w_s}{\partial x^2}\right)$$
$$+ A_{12}\left(\frac{\partial v}{R\partial\theta} + \frac{w_b}{R} + \frac{w_s}{R} + \frac{1}{2}\left(\frac{\partial w_b}{R\partial\theta}\right)^2 + \frac{1}{2}\left(\frac{\partial w_s}{R\partial\theta}\right)^2\right)$$
$$- B_{12}\left(\frac{\partial^2 w_b}{R^2\partial\theta^2}\right) - E_{12}\left(\frac{\partial^2 w_b}{R^2\partial\theta^2}\right) + F_{310}\varphi, \tag{B26}$$

$$N_{\theta\theta} = A_{12}\left(\frac{\partial u}{\partial x} + \frac{1}{2}\left(\frac{\partial w_b}{\partial x}\right)^2 + \frac{1}{2}\left(\frac{\partial w_s}{\partial x}\right)^2\right)$$
$$- B_{12}\left(\frac{\partial^2 w_b}{\partial x^2}\right) - E_{12}\left(\frac{\partial^2 w_s}{\partial x^2}\right)$$
$$+ A_{22}\left(\frac{\partial v}{R\partial\theta} + \frac{w_b}{R} + \frac{w_s}{R} + \frac{1}{2}\left(\frac{\partial w_b}{R\partial\theta}\right)^2 + \frac{1}{2}\left(\frac{\partial w_s}{R\partial\theta}\right)^2\right)$$
$$- B_{22}\left(\frac{\partial^2 w_b}{R^2\partial\theta^2}\right) - E_{22}\left(\frac{\partial^2 w_b}{R^2\partial\theta^2}\right) + F_{310}\varphi, \tag{B27}$$

$$N_{x\theta} = A_{66}\left(\frac{\partial u}{R\partial\theta} + \frac{\partial v}{\partial x} + \left(\frac{\partial w_b}{\partial x} + \frac{\partial w_s}{\partial x}\right)\left(\frac{\partial w_b}{R\partial\theta} + \frac{\partial w_s}{R\partial\theta}\right)\right)$$
$$\left(\frac{\partial w_b}{R\partial\theta} + \frac{\partial w_s}{R\partial\theta}\right)\right) - 2B_{66}\left(\frac{\partial^2 w_b}{R\partial x\partial\theta}\right) - 2E_{66}\left(\frac{\partial^2 w_s}{R\partial x\partial\theta}\right), \tag{B28}$$

$$Q_\theta = A_{44}\left(-\frac{v}{R}\right) - G_{240}\frac{\partial\varphi}{R\partial\theta}, \tag{B29}$$

$$M_{xx} = B_{11}\left(\frac{\partial u}{\partial x} + \frac{1}{2}\left(\frac{\partial w_b}{\partial x}\right)^2 + \frac{1}{2}\left(\frac{\partial w_s}{\partial x}\right)^2\right).$$
$$- D_{11}\left(\frac{\partial^2 w_b}{\partial x^2}\right) - H_{11}\left(\frac{\partial^2 w_s}{\partial x^2}\right)$$
$$+ B_{12}\left(\frac{\partial v}{R\partial\theta} + \frac{w_b}{R} + \frac{w_s}{R} + \frac{1}{2}\left(\frac{\partial w_b}{R\partial\theta}\right)^2 + \frac{1}{2}\left(\frac{\partial w_s}{R\partial\theta}\right)^2\right)$$
$$- D_{12}\left(\frac{\partial^2 w_b}{R^2\partial\theta^2}\right) - H_{12}\left(\frac{\partial^2 w_b}{R^2\partial\theta^2}\right) + F_{311}\varphi, \tag{B30}$$

$$M_{\theta\theta} = B_{12}\left(\frac{\partial u}{\partial x} + \frac{1}{2}\left(\frac{\partial w_b}{\partial x}\right)^2 + \frac{1}{2}\left(\frac{\partial w_s}{\partial x}\right)^2\right)$$
$$- D_{12}\left(\frac{\partial^2 w_b}{\partial x^2}\right) - H_{12}\left(\frac{\partial^2 w_s}{\partial x^2}\right)$$
$$+ B_{22}\left(\frac{\partial v}{R\partial\theta} + \frac{w_b}{R} + \frac{w_s}{R} + \frac{1}{2}\left(\frac{\partial w_b}{R\partial\theta}\right)^2 + \frac{1}{2}\left(\frac{\partial w_s}{R\partial\theta}\right)^2\right)$$
$$- D_{22}\left(\frac{\partial^2 w_b}{R^2\partial\theta^2}\right) - H_{22}\left(\frac{\partial^2 w_b}{R^2\partial\theta^2}\right) + F_{311}\varphi, \tag{B31}$$

$$M_{x\theta} = B_{66}\left(\frac{\partial u}{R\partial\theta} + \frac{\partial v}{\partial x} + \left(\frac{\partial w_b}{\partial x} + \frac{\partial w_s}{\partial x}\right)\left(\frac{\partial w_b}{R\partial\theta} + \frac{\partial w_s}{R\partial\theta}\right)\right)$$
$$- 2D_{66}\left(\frac{\partial^2 w_b}{R\partial x\partial\theta}\right) - 2H_{66}\left(\frac{\partial^2 w_s}{R\partial x\partial\theta}\right), \tag{B32}$$

$$S_{xx} = E_{11}\left(\frac{\partial u}{\partial x} + \frac{1}{2}\left(\frac{\partial w_b}{\partial x}\right)^2 + \frac{1}{2}\left(\frac{\partial w_s}{\partial x}\right)^2\right)$$
$$- H_{11}\left(\frac{\partial^2 w_b}{\partial x^2}\right) - K_{11}\left(\frac{\partial^2 w_s}{\partial x^2}\right)$$
$$+ E_{12}\left(\frac{\partial v}{R\partial\theta} + \frac{w_b}{R} + \frac{w_s}{R} + \frac{1}{2}\left(\frac{\partial w_b}{R\partial\theta}\right)^2 + \frac{1}{2}\left(\frac{\partial w_s}{R\partial\theta}\right)^2\right)$$
$$- H_{12}\left(\frac{\partial^2 w_b}{R^2\partial\theta^2}\right) - K_{12}\left(\frac{\partial^2 w_b}{R^2\partial\theta^2}\right) + F_{31f}\varphi, \tag{B33}$$

$$S_{\theta\theta} = E_{12}\left(\frac{\partial u}{\partial x} + \frac{1}{2}\left(\frac{\partial w_b}{\partial x}\right)^2 + \frac{1}{2}\left(\frac{\partial w_s}{\partial x}\right)^2\right). \tag{B34}$$

$$-H_{12}\left(\frac{\partial^2 w_b}{\partial x^2}\right) - K_{12}\left(\frac{\partial^2 w_s}{\partial x^2}\right)$$

$$S_{\theta\theta} = E_{12}\left(\frac{\partial u}{\partial x} + \frac{1}{2}\left(\frac{\partial w_b}{\partial x}\right)^2 + \frac{1}{2}\left(\frac{\partial w_s}{\partial x}\right)^2\right)$$

$$-H_{12}\left(\frac{\partial^2 w_b}{\partial x^2}\right) - K_{12}\left(\frac{\partial^2 w_s}{\partial x^2}\right) \tag{34}$$

$$+E_{22}\left(\frac{\partial v}{R\partial\theta} + \frac{w_b}{R} + \frac{w_s}{R} + \frac{1}{2}\left(\frac{\partial w_b}{R\partial\theta}\right)^2 + \frac{1}{2}\left(\frac{\partial w_s}{R\partial\theta}\right)^2\right)$$

$$-H_{22}\left(\frac{\partial^2 w_b}{R^2\partial\theta^2}\right) - K_{22}\left(\frac{\partial^2 w_b}{R^2\partial\theta^2}\right) + F_{31f}\,\varphi,$$

$$S_{x\theta} = E_{66}\left(\frac{\partial u}{R\partial\theta} + \frac{\partial v}{\partial x} + \left(\frac{\partial w_b}{\partial x} + \frac{\partial w_s}{\partial x}\right)\left(\frac{\partial w_b}{R\partial\theta} + \frac{\partial w_s}{R\partial\theta}\right)\right) \cdot$$

$$-2H_{66}\left(\frac{\partial^2 w_b}{R\partial x\partial\theta}\right) - 2K_{66}\left(\frac{\partial^2 w_s}{R\partial x\partial\theta}\right), \tag{B35}$$

$$F_{xx} = L_{55}\left(\frac{\partial w_s}{\partial x}\right) - G_{15p}\frac{\partial\varphi}{\partial x}, \tag{B36}$$

$$F_{\theta\theta} = L_{44}\left(\frac{\partial w_s}{R\partial\theta}\right) - G_{24p}\frac{\partial\varphi}{R\partial\theta}, \tag{B37}$$

$$G_x = \frac{e_{15}h}{2}\frac{\partial w_s}{\partial x} + \frac{\in_{11}h}{2}\frac{\partial\varphi}{\partial x}, \tag{B38}$$

$$G_\theta = \frac{e_{24}h}{2\pi}\frac{\partial w_s}{R\partial\theta} - \frac{2e_{24}h}{\pi}\frac{v}{R} + \frac{\in_{22}h}{2}\frac{\partial\varphi}{R\partial\theta}, \tag{B39}$$

$$G_z = \frac{4he_{32}}{\pi}\frac{\partial^2 w_b}{R^2\partial\theta^2} - \frac{h}{2}e_{31}\frac{\partial^2 w_s}{\partial x^2}$$

$$+\frac{2h}{\pi}e_{31}\left(\frac{\partial^2 w_b}{\partial x^2} + \frac{\partial^2 w_s}{\partial x^2}\right) + \frac{\pi^2\in_{33}}{2h}\varphi - \frac{he_{32}}{2}\frac{\partial^2 w_b}{R^2\partial\theta^2} \tag{B40}$$